

Economic Geology

BULLETIN OF THE SOCIETY OF ECONOMIC GEOLOGISTS

VOL. 99

June–July 2004

No. 4

The Late Cretaceous Donlin Creek Gold Deposit, Southwestern Alaska: Controls on Epizonal Ore Formation

RICHARD J. GOLDFARB,[†]

U.S. Geological Survey, Box 25046, Denver Federal Center, Denver, Colorado 80225

ROBERT AYUSO,

U.S. Geological Survey, 12201 Sunrise Valley Drive, Mail Stop 954, Reston, Virginia 20192

MARTI L. MILLER,

U.S. Geological Survey, 4200 University Drive, Anchorage, Alaska 99508-4667

SHANE W. EBERT,

Mineral Deposit Research Unit, Department of Earth and Ocean Sciences, University of British Columbia, 6339 Stores Road, Vancouver, British Columbia V6T 1Z4

ERIN E. MARSH,

U.S. Geological Survey, Box 25046, Denver Federal Center, Denver, Colorado 80225

SCOTT A. PETSSEL,

NovaGold Resources Inc., 4420 Taku Blvd., Juneau, Alaska 99801

LANCE D. MILLER,

Juneau Economic Development Council, 612 W. Willoughby, Juneau, Alaska 99801

DWIGHT BRADLEY,

U.S. Geological Survey, 4200 University Drive, Anchorage, Alaska 99508-4667

CRAIG JOHNSON,

U.S. Geological Survey, Box 25046, Denver Federal Center, Denver, Colorado 80225

AND WILLIAM MCCLELLAND

Department of Geological Sciences, University of Idaho, Moscow, Idaho 83844

Abstract

The Donlin Creek gold deposit, southwestern Alaska, has an indicated and inferred resource of approximately 25 million ounces (Moz) Au at a cutoff grade of 1.5 g/t. The ca. 70 Ma deposit is hosted in the Late Cretaceous Kuskokwim flysch basin, which developed in the back part of the arc region of an active continental margin, on previously accreted oceanic terranes and continental fragments. A hypabyssal, mainly rhyolitic to

[†] Corresponding author: email, Goldfarb@usgs.gov

rhyodacitic, and commonly porphyritic, 8- × 3-km dike complex, part of a regional ca. 77 to 58 Ma magmatic arc, formed a structurally competent host for the mineralization. This deposit is subdivided into about one dozen distinct prospects, most of which consist of dense quartz ± carbonate veinlet networks that fill north-northeast-striking extensional fractures in the northeast-trending igneous rocks. The sulfide mineral assemblage is dominated by arsenopyrite, pyrite, and, typically younger, stibnite; gold is refractory within the arsenopyrite. Sericitization, carbonatization, and sulfidation were the main alteration processes.

Fluid inclusion studies of the quartz that hosts the resource indicate dominantly aqueous ore fluids with also about 3 to 7 mol percent CO₂ ± CH₄ and a few tenths to a few mole percent NaCl + KCl. The gold-bearing fluids were mainly homogeneously trapped at approximately 275° to 300°C and at depths of 1 to 2 km. Some of the younger stibnite may have been deposited by late-stage aqueous fluids at lower temperature. Measured δ¹⁸O values for the gold-bearing quartz range between 11 and 25 per mil; the estimated δ¹⁸O fluid values range from 7 to 12 per mil, suggesting a mainly crustally derived fluid. A broad range of measured δD values for hydrothermal micas, between -150 and -80 per mil, is suggestive of a contribution from devolatilization of organic matter and/or minor amounts of mixing with meteoric fluids. Gold-associated hydrothermal sulfide minerals are characterized by δ³⁴S values mainly between -16 and -10 per mil, with the sulfur derived from diagenetic pyrite and organic matter within the flysch basin. A smaller group of δ³⁴S measurements, which shows values as depleted as -27 per mil, suggests a different local sulfur reservoir in the basin for the later hydrothermal episode dominated by stibnite. Initial ε_{Nd} of -8.7 to -3.1 and ⁸⁷Sr/⁸⁶Sr measurements of 0.706 to 0.709 for the ore-hosting dikes also indicate a crustal reservoir for some of the Late Cretaceous magmatism. Overlapping lead isotope data for these intrusive rocks and for sulfide minerals suggest a crustal contribution for the lead in both.

Copper- and gold-bearing stockwork veinlets in hornfels occur at Dome, a prospect located at the northern end of the Donlin Creek deposit. These stockworks are cut by the younger auriferous gold veins that define the main Donlin Creek gold mineralization. Highly saline, gas-rich, heterogeneously trapped fluids deposited the stockworks at temperatures approximately 100°C hotter than those of the main gold-forming event at Donlin Creek. The genetic relationship of the Dome prospect to the main Donlin Creek gold resource is equivocal.

The epizonal Donlin Creek deposit shows affinities to the gold systems interpreted by various workers as orogenic or intrusion related; it shows important differences from typical epithermal and Carlin-like deposits. The ore-forming fluids were derived by either broad-scale metamorphic devolatilization above rising mantle melts or exsolution from a magma that was dominated by a significant flysch melt component.

Introduction

THE DONLIN CREEK gold deposit is a recently defined low-grade, large-tonnage resource in the Kuskokwim Mountains of southwestern Alaska (Fig. 1). The deposit is located about 450 km west-northwest of Anchorage and 20 km from the Kuskokwim River. The indicated and inferred resource has been recently increased to 25.4 Moz Au at a 1.5 g/t Au cutoff grade (Placer Dome press release, 4/9/03). The resource is open at depth and along strike. Low gold prices, the refractory nature of the potential ore, and the relatively remote location have collectively hindered development of the property to date. Nevertheless, the property represents a world-class gold resource of great interest and the largest lode gold deposit in the northern Cordillera of western North America.

The Kuskokwim Mountains region (Figs. 1–2A) is characterized by rolling hills that reach maximum elevations of 1,000 m. The dominant bedrock is very weakly metamorphosed Upper Cretaceous basin fill, which is widely intruded by Late Cretaceous to earliest Tertiary igneous rocks (Figs. 1, 3). Mineral production in this region has historically been from scattered placer gold accumulations that have yielded almost 3.5 Moz Au (Bundtzen and Miller, 1997; Swainbank et al., 2001). Almost one-half of this placer production has come from the Iditarod district, where the auriferous quartz veins of the Golden Horn deposit, hosted by the Black Creek stock, provided a significant lode source (Bull, 1988).

Three general groups of metallic ore deposits are recognized in this region (Fig. 1): (1) small, epithermal mercury-antimony deposits (e.g., Red Devil) that cut Cretaceous clastic rocks and mafic dikes (Sainsbury and MacKevett, 1965;

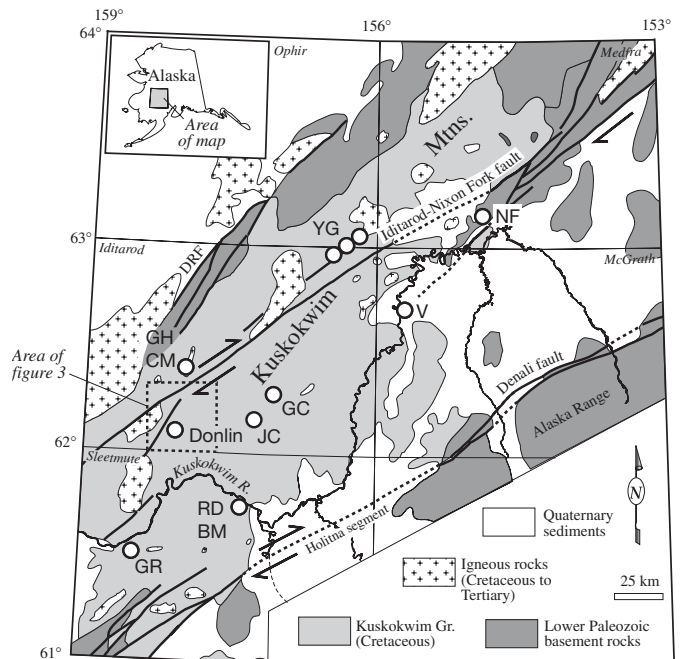


FIG. 1. Location of the Donlin Creek gold deposit, Kuskokwim region, southwestern Alaska. Other metallic mineral deposits in the region include (1) epithermal mercury-antimony deposits at Red Devil (RD) and Barometer Mountain (BM); (2) other gold-rich stockworks and veins at Golden Horn (GH), Chicken Mountain (CM), Ganes-Yankee Creek (YG), Julian Creek (JC), Granite Creek (GC), Vinasale (V), Stuyahok (not shown; 200 km SW of Donlin Creek), and Gold Run (GR); and (3) calcic, gold-rich copper skarns at Nixon Fork (NF). After Miller et al. (2002).

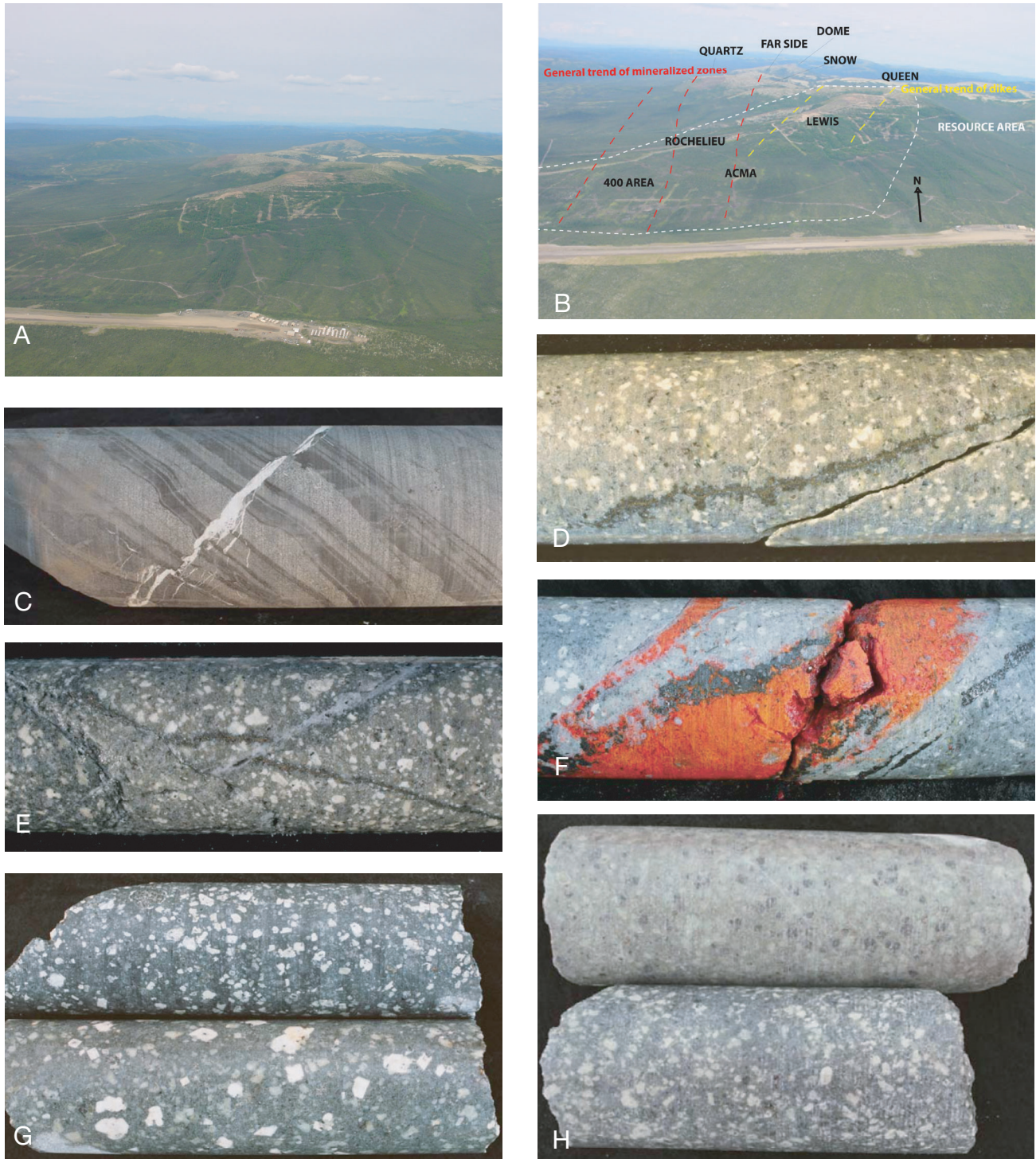


FIG. 2. A. Overview photo of the Donlin Creek deposit area that is centered on a series of topographic domes in the rolling hills that define the Kuskokwim Mountains of southwestern Alaska. B. Most of the mineralization at the Donlin Creek gold deposit occurs in a series of drilled prospects within an 8-km-long, NNE-trending igneous dike complex. The gold resource is located in the more southerly prospects. C. Typical rhythmically banded siltstone and graywacke of the Kuskokwim Group, which is the country rock to the dike complex. D. Early, thin pyrite veinlet cutting rhyodacite porphyry. E. Quartz vein with gold-bearing arsenopyrite selvage cutting earlier pyrite vein. F. Late veinlet with realgar, native arsenic, and stibnite that overprints earlier auriferous arsenopyrite event. G. Graphite clots in coarse-grained rhyodacite host that often give a bluish tinge to the intrusive rocks. H. Typical rhyodacite host rock with strong ankerite (top) and kaolinite (bottom) alteration. Some of the photos reproduced from unpublished report of Piekenbrock and Petsel (2003).

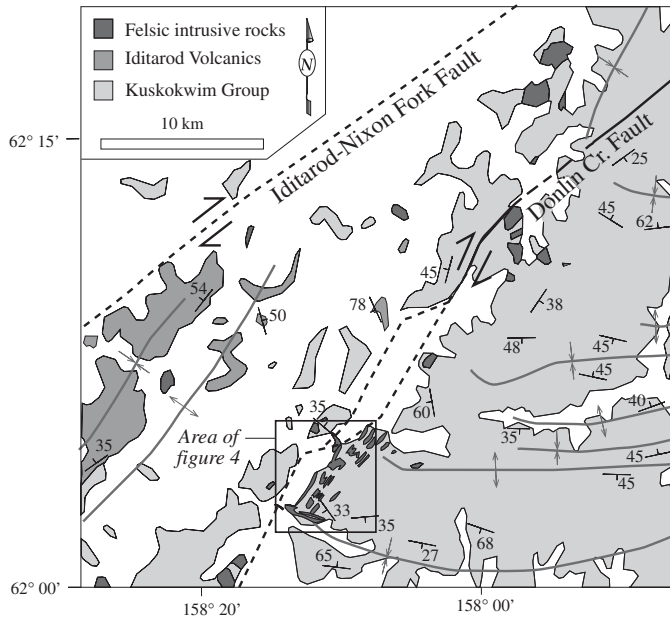


FIG. 3. Local geology of the area surrounding the Donlin Creek deposit, southwestern Alaska, after mapping of Miller and Bundtzen (1994). The deposit occurs in a structurally complex region of the Kuskokwim basin, where it is hosted by a granite dike complex located a few kilometers to the east of the Donlin Creek fault and on the western edge of a series of regional folds.

Gray et al., 1997); (2) gold-rich stockworks and veins that are hosted by multiphase volcanic-plutonic complexes (e.g., Golden Horn) or are spatially associated with granite porphyry dikes (e.g., Donlin Creek) or stocks (e.g., Vinasale Mountain, Shotgun), which intrude the clastic sequence (Bundtzen and Miller, 1997); and (3) calcic, gold-rich copper skarns (e.g., Nixon Fork) where plutons intrude adjacent carbonate platform rocks in allochthonous terrane blocks (Newberry et al., 1997). The specific genetic associations between all three groups of deposits, as well as the igneous rocks, remain enigmatic, although all ore systems and much of the magmatism reflect an important broad thermal event in southwestern Alaska at ca. 70 Ma (Bundtzen and Miller, 1997; Goldfarb, 1997; Miller et al., 2002). An obvious possibility is that the epithermal mercury-antimony deposits of the Kuskokwim Mountains may be distal parts of zoned, gold-rich hydrothermal systems.

Small-scale placer mining along Crooked Creek (Fig. 4), downstream from the newly defined Donlin Creek lode resource, has taken place intermittently for almost 100 yr (e.g., Cady et al., 1955) but with total production of <50,000 oz Au (Ebert et al., 2000b). The gold from these placers has the highest average fineness among any of the placers in this part of southwestern Alaska (approx 940; Bundtzen et al., 1985). Discontinuous, thin quartz-calcite veins, some associated with massive stibnite, were historically prospected on the

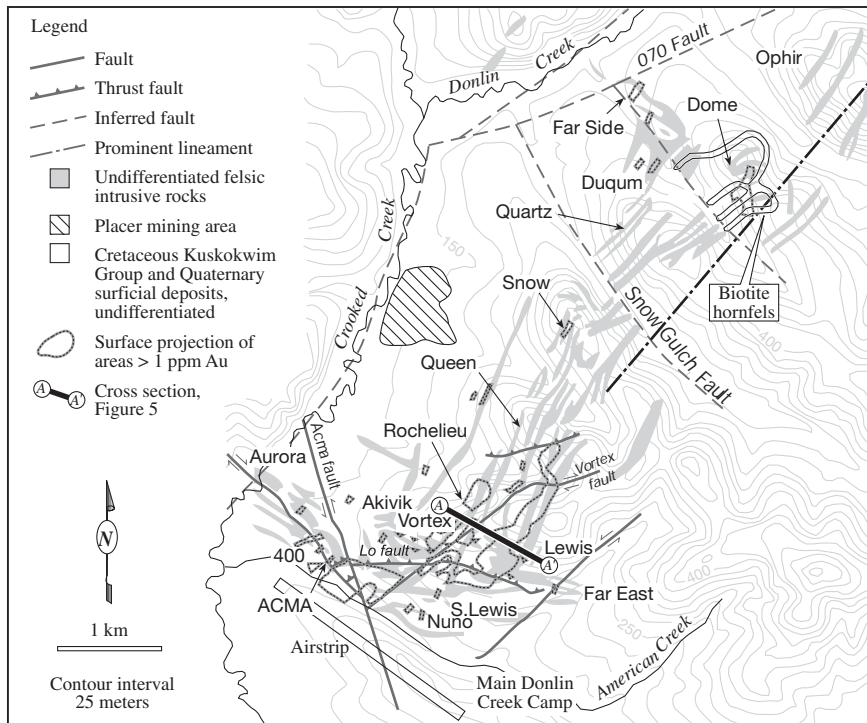


FIG. 4. The Donlin Creek gold deposit is comprised of the Ophir, Dome, Duqum, Far Side, Quartz, Snow, Queen, Rochelieu, Lewis, South Lewis, Far East, Nuno, Vortex, Aurora, Akivik, ACMA, and 400 prospects, with the present resource confined to the southernmost part of the deposit. The deposit is defined by an 8- × 3-km zone of NNE-striking narrow veins, which are mainly hosted by extensional fractures within and adjacent to a NE-trending zone of granite porphyry dikes and sills that were emplaced immediately east of the Donlin Creek fault. Recent interpretation of air photos, aeromagnetic data, and resistivity data suggests that the Donlin Creek fault is not as straight as previously mapped but instead has a stepped pattern. The southern part of the rhomb-shaped stepover (see Fig. 3) is an ENE-striking fault referred to as the “070 fault” by some workers (e.g., Ebert et al., 2000b). Surficial geology as defined by Bundtzen and Miller (1997) and Piekenbrock and Petsel (2003). Cross section A-A’ is presented in Figure 7.

hillside along and above Snow Gulch (Fig. 4) but with no further development.

Extensive trenching by Westgold Exploration and Mining Company was undertaken on the property in the late 1980s. A reconnaissance examination of the stibnite-rich zones at this same time indicated high oxygen isotope values for the veins that contrasted with those of typical epithermal mineral deposits (Goldfarb et al., 1990), and measurements of as much as 7 ppm Au in the veins (Gray et al., 1990), which further suggested to these workers that the stibnite-rich veins could be the shallowly exposed part of an important gold-enriched lode system. Beginning in 1995, and continuing for about 5 yr, Placer Dome Inc. and NovaGold Resources Inc. carried out extensive drilling programs and geologic studies of the Donlin Creek deposit, which led to the presently defined resource. Recently, Placer Dome Inc. has become the major owner of the deposit and is presently conducting a major premining feasibility drilling program. Initial results are favorable for possible development of an open-pit mine at a 2 g/t Au cutoff.

The first descriptions of the Donlin Creek deposit were by Dodd (1996), Ebert et al. (2000a, b), and Szumigala et al. (2000). In this paper, we thus summarize some of main geologic conclusions from these studies and then combine these with many of our own observations. We present the first detailed isotope and fluid inclusion data to help characterize the ore-forming fluids and examine the petrogenesis of igneous rocks that are spatially associated with the ores. Finally, we synthesize this information into a model that places the origin of the Donlin Creek deposit into the most recent tectonic framework for southwestern Alaska.

Regional Geology

Upper Cretaceous Kuskokwim Group

The Kuskokwim region of southwestern Alaska (Fig. 1) is predominantly underlain by rocks of the Upper Cretaceous Kuskokwim Group. These include coarse- through fine-grained clastic rocks that have a diversity in provenance and which reach a maximum thickness of >10 km (Decker et al., 1994). Minor, interbedded andesitic tuff and flows are also present near the top of the sequence (Miller and Bundtzen, 1994) and may represent initiation of volcanism that later culminated in widespread Late Cretaceous and early Tertiary igneous activity (see below). Fossil ages constrain sedimentation to Cenomanian to probable Campanian (ca. 95–77 Ma; Miller et al., 2002). In the region of the Donlin Creek gold deposit, rocks are no older than Turonian (ca. 91 Ma; Miller and Bundtzen, 1994).

The rocks of the Kuskokwim Group filled a northeast-trending, strike-slip basin that subsided between a series of amalgamated terranes. The underlying basement terranes include a Mesozoic oceanic arc dominated by marine volcanic and sedimentary rocks, a Paleozoic passive-margin sequence of mainly platform and deep-water carbonate rocks, and a fragment of Proterozoic continental basement consisting of amphibolite and metaplutonic rocks (Miller et al., 1991; Decker et al., 1994). Regional deformation was initiated in the Late Cretaceous. Exposed parts of the Kuskokwim Group show evidence of only the lowest grades of regional burial metamorphism.

Late Cretaceous to early Tertiary magmatism

Igneous activity was coeval with later periods of Late Cretaceous sedimentation in the Kuskokwim basin and also continued into the early Tertiary. About 20, calc-alkaline, mainly intermediate composition volcanic-plutonic complexes intrude and overlie rocks of the Kuskokwim Group (Miller et al., 1989, Moll-Stalcup, 1994). These complexes, as large as 650 km² in exposed area, are dominated by tuffs, flows, and composite comagmatic plutons of monzonite to granodiorite composition. Most ages for the volcanic rocks are 76 to 63 Ma, whereas the associated intrusions yield dates between 71 and 66 Ma (Miller and Bundtzen, 1994; Decker et al., 1995; Bundtzen and Miller, 1997). About one-half of these complexes contain subeconomic Au-, Cu-, Sn-, and/or W-rich greisenization or lower temperature and, in some cases, economic, auriferous stockwork systems (e.g., Golden Horn). Additional coeval magmatism includes extensive ($\leq 5,000$ km²) subaerial andesitic volcanic fields, which, at the present level of exposure, lack associated intrusions and metalliferous hydrothermal systems.

Volumetrically minor mafic to intermediate latest Cretaceous dikes are scattered throughout the Kuskokwim region. These are characteristically silica-carbonate altered and are spatially associated with much of the mercury- and antimony-rich epithermal mineralization.

Felsic to intermediate hypabyssal granite (sometimes extending to granodiorite in composition) porphyry dikes and plugs are also ca. 70 to 65 Ma in age (Miller and Bundtzen, 1994), although their overall genetic association with the volcanic-plutonic complexes is uncertain. These intrusions characteristically show a spatial association with many lode and placer gold deposits (e.g., Donlin Creek, Vinasale Mountain). Szumigala (tables 2-2 and 2-3, 1993) obtained detailed geochemical and mineralogical data for typical examples of all the igneous units.

Petrogenetic studies by Moll-Stalcup (1994) suggested that volcanic rocks and volcanic-plutonic complexes of southwestern Alaska are part of a very broad, LREE-enriched, subduction-related arc. Magmas have undergone significant amounts of fractionation and show evidence for extensive crustal interaction. The approximately coeval suite of hypabyssal dikes, sills, and stocks, on the other hand, are peraluminous and locally garnet bearing, which suggests they likely represent melted crust (Miller and Bundtzen, 1994). New radiogenic isotope data presented in this paper (see below) confirm that some magmas, such as those spatially associated with gold ores, are definitely not mantle derived and place additional constraints on their potential source(s).

Regional structures

The Donlin Creek deposit lies between two major dextral strike-slip faults—the Holitna segment of the Denali fault system and the Iditarod-Nixon Fork fault system (Fig. 1). Miller et al. (2002) summarized the tectonic history of these two regional structures in southwestern Alaska. The Holitna segment shows about 134 km of right-lateral offset since initiation of basin sedimentation; rocks along the Iditarod-Nixon Fork fault have been offset >90 km right laterally since about 58 Ma, but the fault was also active at least as far back as 90

Ma. The Late Cretaceous strike-slip motion is best interpreted as a product of oblique subduction prior to the oroclinal bending of Alaska (Miller et al., 2002).

The Donlin Creek gold deposit is located along a splay (informally named the Donlin Creek fault; Fig. 3) of the Iditarod-Nixon Fork fault system and about 10 km to the southeast of the main branch of the fault. High-angle, northeast-striking faults in this system form a broad belt about 10 to 20 km in width. In the Yankee Creek-Ganes Creek area (Fig. 1), about 90 km northeast of Donlin Creek, another splay of the Iditarod-Nixon Fork fault system is associated with an additional mineralized hypabyssal dike swarm. Miller and Bundtzen (1994) suggested that the two mineralized areas were originally together and have been offset dextrally by the master fault. If so, then initially the gold resource at the Donlin Creek deposit was even larger than that recognized in the present-day configuration of southwestern Alaska.

Regional folds of several orientations are recognized in the Kuskokwim region (Fig. 3). The main folding probably took place soon after basin sedimentation, because regional structures are commonly truncated by the Late Cretaceous volcanic-plutonic complexes. East- to west-trending, open to tight folds, which have amplitudes of 2 to 3 km, are abundant to the east of the Donlin Creek deposit (Miller and Bundtzen, 1994; Fig. 3). The Donlin Creek deposit is localized in a structurally complex area, where these folds are truncated to the west by the Donlin Creek fault.

Local Geology of the Donlin Creek Deposit

The Donlin Creek deposit (Figs. 2B, 4) is comprised of more than one dozen drilled prospects (Ophir, Dome, Duqum, Far Side, Quartz, Snow, Queen, Rochelieu, Lewis, South Lewis, Far East, Nuno, Akivik, Vortex, Aurora, ACMA, and 400) within and adjacent to an 8-km-long, northeast-trending rhyolite and/or rhyodacite dike complex (Bundtzen and Miller, 1997; Szumigala et al., 2000). The defined gold resource is contained in the ACMA-Lewis area at the southern end of the deposit and dike complex. The country rocks at the deposit are interbedded graywacke and shale of the Kuskokwim Group (Fig. 2C) that strike roughly northwest and dip 35° to 50° to the southwest. The coarser grained strata are rich in metamorphic lithic fragments, but igneous and sedimentary rock fragments are also locally abundant. The finer grained units sometimes contain fine, syngenetic pyrite and coaly leaf and stem fragments (Miller and Bundtzen, 1994). These shales are the more common sedimentary unit in the area of the gold resource and are the main country rock for the dike complex. The sedimentary rocks are silicified close to the dikes, and at the northern end of the deposit, in the vicinity of the Dome prospect, a well-developed biotite hornfels is cut by the dikes (Fig. 4).

The 8- × 3-km swarm of mineralized, discordant, mainly felsic porphyry dikes, with lesser sills, at the Donlin Creek deposit (Figs. 2B, 4) was emplaced within a complexly faulted area. Individual dikes average 3 to 20 m in width, and contacts with the country rock are often very irregular along strike. Based on limited analyses, Bundtzen and Miller (1997) defined these as evolved, calcic, peraluminous hypabyssal bodies with high silica (74.1% SiO₂) and aluminum (14.5% Al₂O₃)

contents. On a normative QAPF diagram, they classified the dikes as alkali-quartz granite. Additional analyses of the igneous rocks suggest lower SiO₂ (65–72%), typically with about 0.2 to 2.7 percent CaO, 3 to 4 percent K₂O, and 2 to 4 percent Na₂O (Szumigala et al., 2000; S. Ebert, unpub. data). Phenocrysts (≤15–20 mm) are dominated by quartz, plagioclase, and K-feldspar, accompanied by lesser biotite and muscovite, and rare garnet (Miller and Bundtzen, 1994).

Company geologists have attempted to visually classify the igneous rocks at the deposit into five petrographic groups, which are summarized by Szumigala et al. (2000). Most of the dikes and sills are defined as either aphanitic rhyodacite porphyry or crystalline rhyodacite porphyry; less common are rhyolite porphyry and fine-grained rhyodacite porphyry. There are also rare, relatively early, lamprophyre dikes. Ebert et al. (2000a) detail the differences in mineralogy between the various rhyolite and rhyodacite phases; importantly, all compositions are altered and mineralized by the subsequent hydrothermal activity. It is also significant to note that, although the felsic igneous rocks are referred to as rhyolite and rhyodacite by local workers, they are, in actuality, shallowly emplaced intrusive rocks belonging to the regional suite of granite porphyry dikes and stocks described by Miller and Bundtzen (1994).

Local structure

The Donlin Creek deposit is located in a structurally complex area between two regional-scale strike-slip faults (Fig. 1). North-south en echelon folds near these master faults are clearly related to the wrench-fault environment (Miller et al., 2002). However, in the region between the master faults, folds trend roughly east-west and the structural regime does not show any obvious connections to wrench faulting. One explanation offered by Miller et al. (2002) is that deformation was partitioned on a regional scale, as is common above oblique subduction zones. Regardless of the explanation, the Donlin Creek splay is the boundary between these substantially different structural domains. The deposit is located just 1 to 2 km southeast of the Donlin Creek fault (Fig. 3).

The structural geology of the Donlin Creek deposit has been described by Ebert et al. (2000a, b) and Miller et al. (2000), mainly through study of core samples and limited surface exposures. Subsequent observations by company geologists during recent drilling programs (Piekenbrock and Petsel, 2003) have furthered understanding of the structural geology. The gold occurs in dilatant veins, which are the youngest structures to have formed during a closely timed series of events. The following structural elements are recognized, listed in chronological order as revealed by crosscutting relationships:

1. The oldest documented structures are approximately east-west folds and associated southerly directed thrusts in rocks of the Kuskokwim Group. The low-angle thrusting appears to be focused along bedding planes within the varied sedimentary facies (Piekenbrock and Petsel, 2003).

2. At ca. 70 Ma, north-northeast-striking dikes and associated west-northwest-striking sills were emplaced in multiple pulses. Some of the dikes are cut by thrusts, indicating an overlap in the age of these structures.

3. Crosscutting northeast- and northwest-striking high-angle faults (Fig. 4) developed soon after the thrusts and may have also been active during igneous activity.

4. Finally, the gold-bearing north-northeast–striking (Fig. 5) extensional fractures formed and cut both the igneous rocks and all fault generations (Ebert et al., 2000a; Miller et al., 2000). These extensional structures are preferentially concentrated in the relatively competent igneous rocks and coarser grained sedimentary rocks.

Age of igneous activity

Previous K-Ar dating of magmatic biotite and muscovite phenocrysts from three unaltered dikes, just a few kilometers east and west of the Donlin Creek deposit, yielded dates between 70.9 ± 2.1 and 65.1 ± 2.0 Ma (Miller and Bundtzen, 1994). However, because of the broad range in these dates, inherent precision problems with the K-Ar technique, and the possibility of some argon loss from magmatic minerals by superimposed hydrothermal activity, we employed more precise U-Pb techniques for absolute age constraints.

Zircons were separated for U-Pb analysis from a rhyodacite dike sample collected at about a 5-m depth in drill hole LT-96-33 from the Lewis prospect. Three of the five fractions analyzed (Table 1, Fig. 6) are discordant due to the combined effects of lead loss and inherited components. A crystallization age of 69.2 ± 0.5 Ma is inferred for this sample based on two fractions of strongly abraded zircon that yield concordant to nearly concordant analyses. This age is consistent with the older age of the previously reported K-Ar range and suggests that younger K-Ar ages could reflect argon loss.

A second sample was collected from a dike at the Dome prospect. The sample is a malachite-stained rhyolite dike exposed in one of the trenches at the prospect. Zircons from this sample yielded two discordant fractions, which reflect the presence of Precambrian inherited components and two concordant fractions that yield an age of 66.5 ± 0.5 Ma.

In addition to our U-Pb work, recent igneous rock $^{40}\text{Ar}/^{39}\text{Ar}$ dates, with well-defined plateaus (e.g., Szumigala et al., 2000, fig. 4) have been obtained from the Queen prospect. These

include a biotite plateau age of 70.3 ± 0.2 Ma for a rhyolite porphyry dike, as well as a biotite plateau age of 72.6 ± 0.9 Ma, and a whole-rock age of 74.4 ± 0.8 Ma for a mafic dike (Szumigala et al., 2000). It is uncertain as to whether these are the true crystallization ages of the igneous rocks or whether they reflect cooling through the mica closure temperatures. We favor the former possibility; i.e., that there was a protracted period of magmatism in the Donlin Creek area that may have lasted for 3 to 5 m.y. (ca. 74.4 ± 0.8 – 70.3 ± 0.2 Ma) or even longer when the above younger U-Pb dates are considered. The shallow-level emplacement of the sills and dikes into low-grade (e.g., already at or below biotite blocking temperatures) metamorphic rocks argues against a lengthy period of cooling for any of the intrusions, such that the plateau ages are likely to approximate the mineral crystallization ages.

Hydrothermal alteration and gold mineralization within the Donlin Creek resource

The gold resource at the Donlin Creek deposit occurs in north-northeast–striking (average 012° – 020°), steeply dipping (generally $>70^\circ$ SE), thin veins that fill brittle, extensional fractures in the dikes and sills within the ACMA-Lewis prospect area (Fig. 7). However, some mineralization does occur along dike-sedimentary rock contacts and in relatively competent sedimentary rock beds. The north-northeast trend to the mineralized veins is consistent throughout the entire deposit and is not just restricted to the defined resource area (Fig. 5). Most of the veins are a few centimeters wide, although rare veins may be a few decimeters in width. Maximum vein lengths in trenches are 7 m. Local epizonal (i.e., at conditions of 150° – 300°C and <6 km; Groves et al., 1998) features include abundant drusy quartz-lined cavities, banding, and cockade and bladed textures. Szumigala et al. (2000) noted that ore zones tend to steepen and form high-grade ore shoots where they cut the more competent igneous rocks.

The ACMA-Lewis area gold-bearing veins are dominated by gray and clear quartz, with subordinate dolomite and ankerite, and locally as much as 5 percent illite. Pyrite,

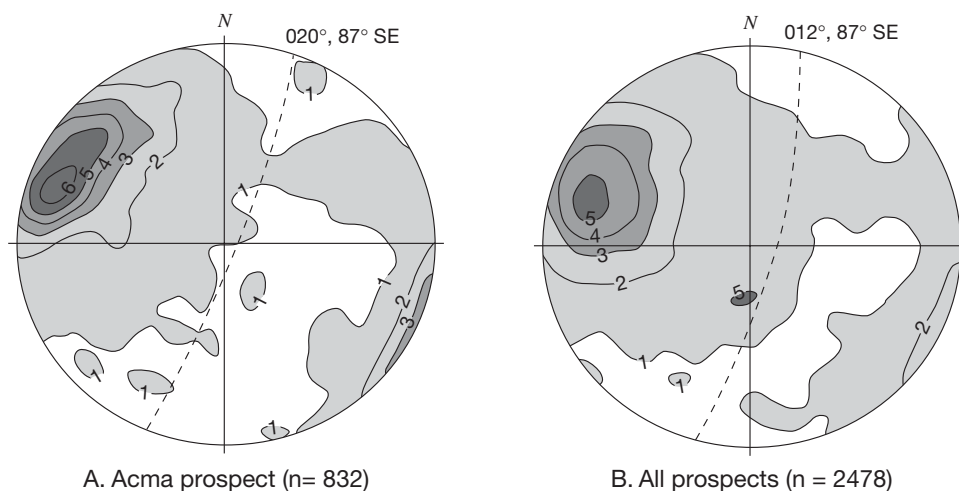


FIG. 5. Stereonet of mineralized veins, displayed as contour plots in percent of points per each one percent of area, showing the strong NNE strike to the dominant ore-bearing fracture set. Data are for (A) 832 veins from the main resource area at the ACMA prospect and (B) 2,478 veins over the entire deposit area.

TABLE 1. U-Pb Isotope Zircon Data and Apparent Ages

Sample	Fraction size ¹ (μm)	Wt (mg)	Concentration (ppm)		Isotopic composition ³			Apparent ages ⁴ (Ma)			Th-corrected ages ⁵ (Ma)	
			U	Pb ²	²⁰⁶ Pb	²⁰⁶ Pb	²⁰⁶ Pb	²⁰⁶ Pb ^o	²⁰⁷ Pb ^o	²⁰⁷ Pb ^o	²⁰⁶ Pb ^o	²⁰⁷ Pb ^o
					²⁰⁴ Pb	²⁰⁷ Pb	²⁰⁸ Pb	²³⁸ U	²³⁵ U	²⁰⁶ Pb ^o	²³⁸ U	²⁰⁶ Pb ^o
Sample 96AM105 Lewis prospect, rhyodacite dike												
a	45-63	0.1	944	10.7	8,080 \pm 19	17.171	17.208	76.0	89.6 \pm 0.2	470	76.0 \pm 0.2	467 \pm 2
b	63-80A	0.2	1,076	10.6	10,445 \pm 20	19.835	18.592	66.7	68.9 \pm 0.1	148	66.8 \pm 0.1	146 \pm 2
c	80-100A	0.2	966	9.5	9,808 \pm 21	20.024	19.713	66.8	68.3 \pm 0.1	121	66.9 \pm 0.1	118 \pm 2
d	100-350A	0.2	906	9.2	9,638 \pm 17	20.383	18.309	69.0	69.2 \pm 0.1	76	69.0 \pm 0.1	73 \pm 2
e	100-350A	0.2	873	8.9	9,929 \pm 18	20.429	18.704	69.1	69.2 \pm 0.1	73	69.2 \pm 0.1	70 \pm 2
Sample 96AM106 Dome prospect, rhyolite dike												
a	45-63	0.1	835	8.4	6,868 \pm 17	19.596	18.263	68.4	70.5 \pm 0.2	143	68.5 \pm 0.1	140 \pm 3
b	63-80A	0.2	86	9.9	3,875 \pm 6	11.135	8.852	690.1	864.5 \pm 1.8	1,343	690.2 \pm 1.3	1,342 \pm 1
c	80-100A	0.2	646	6.2	5,481 \pm 7	19.958	20.842	66.2	66.4 \pm 0.1	71	66.3 \pm 0.1	68 \pm 2
d	100-350A	0.2	723	7.0	11,425 \pm 48	20.527	25.370	66.4	66.5 \pm 0.2	71	66.5 \pm 0.1	68 \pm 3

¹ a, b, etc. designate conventional multigrain fractions; A designates fractions abraded to 30 to 60% of original mass; zircon fractions are nonmagnetic on Frantz magnetic separator at 1.8 amps, 15° forward slope, and side slope of 1°

² Pb^o is radiogenic Pb

³ Reported ratios corrected for fractionation ($0.125 \pm 0.038\%$ /amu) and spike Pb; ratios used in age calculation were adjusted for 2 pg of blank Pb with isotopic composition of $^{206}\text{Pb}/^{204}\text{Pb} = 18.6$, $^{207}\text{Pb}/^{204}\text{Pb} = 15.5$, and $^{208}\text{Pb}/^{204}\text{Pb} = 38.4$, 2 pg of blank U, $0.25 \pm 0.049\%$ /amu fractionation for UO_2 , and initial common Pb with isotopic composition approximated from Stacey and Kramers (1975) with an assigned uncertainty of 0.1 to initial $^{207}\text{Pb}/^{204}\text{Pb}$ ratio

⁴ Uncertainties reported as 2σ ; error assignment for individual analyses follows Mattinson (1987) and is consistent with Ludwig (1991); an uncertainty of 0.2% is assigned to the $^{206}\text{Pb}/^{238}\text{U}$ ratio based on our estimated reproducibility unless this value is exceeded by analytical uncertainties; calculated uncertainty in the $^{207}\text{Pb}/^{206}\text{Pb}$ ratio incorporates uncertainty due to measured $^{204}\text{Pb}/^{206}\text{Pb}$ and $^{207}\text{Pb}/^{206}\text{Pb}$ ratios, initial $^{207}\text{Pb}/^{204}\text{Pb}$ ratio, and composition and amount of blank; linear regression of discordant data utilized Ludwig (1992); decay constants used: $^{238}\text{U} = 1.5513 \text{ E-10}$, $^{235}\text{U} = 9.8485 \text{ E-10}$, $^{238}\text{U}/^{235}\text{U} = 137.88$

⁵ A $75 \pm 25\%$ efficiency in ^{230}Th exclusion during zircon crystallization is assumed and $^{207}\text{Pb}/^{206}\text{Pb}$ and $^{206}\text{Pb}/^{238}\text{U}$ ratios have been adjusted accordingly; age assignments presented are derived from the Th-corrected ratios

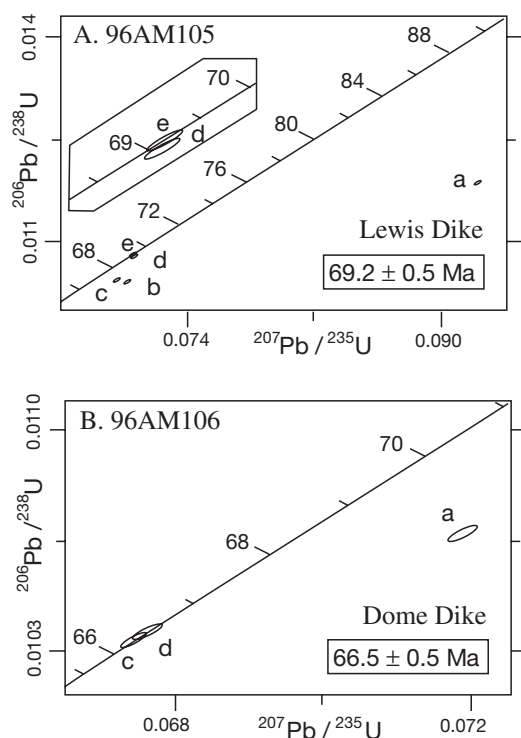


FIG. 6. U-Pb concordia diagram for zircons from least altered rhyodacite and rhyolite dike samples from the Lewis and Dome prospects at the Donlin Creek gold deposit. A thorium-corrected age of $69.2 \pm 0.5 \text{ Ma}$ is interpreted as representative of time of preore dike emplacement at Lewis, whereas the age for the Dome dike is $66.5 \pm 0.5 \text{ Ma}$. Letters a, b, c, d, and e refer to different zircon fractions. Data for fraction b, sample 96AM106, have not been included.

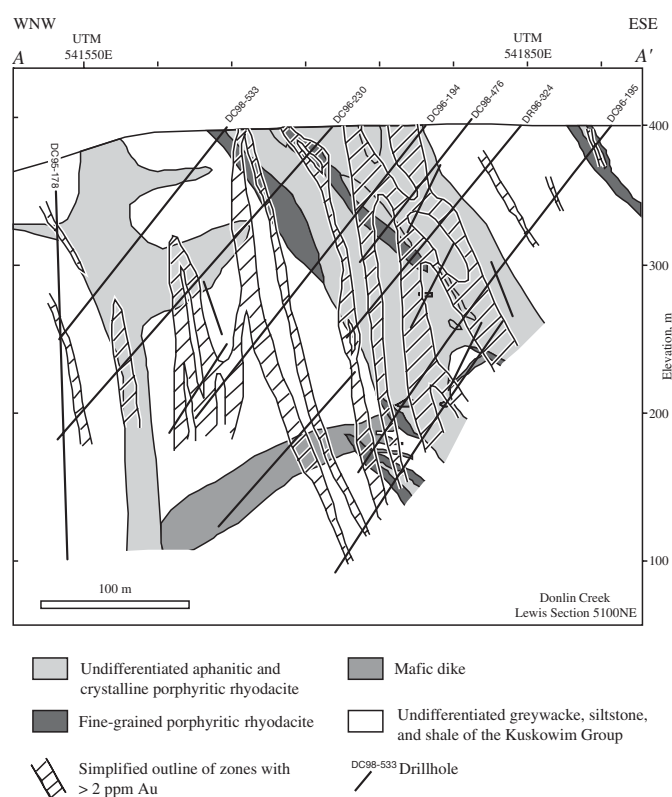


FIG. 7. A cross section at 5100NE through the Lewis prospect, showing the slight discordance between ore zones (>2 ppm Au) and the dike/sill complex. Figure generalized from Ebert et al. (2000a-b). Location of section shown in Figure 4.

arsenopyrite, and stibnite are the dominant sulfide minerals and may comprise as much as 3 to 5 percent of the gold-rich zones. Some pyrite occurs as relatively early, low-grade, thin veinlets (Fig. 2D), with only minor quartz and ankerite, which are then cut by the auriferous and arsenopyrite-bearing quartz veins (Fig. 2E). The sulfide minerals are relatively fine grained, generally $<50\ \mu\text{m}$ in diameter, and gold-bearing arsenopyrite typically occurs as needles. Stibnite is locally present as coarse laths that exceed 1 cm in length (particularly in the area between Snow and ACMA-Lewis), but it more typically appears as late open-space fillings and fracture coatings. Some of these late fractures also contain crystalline realgar, orpiment, and rare native arsenic (Fig. 2F). Minor cinnabar and fine-grained graphite are present, most commonly observed locally in paragenetically late thin veins or in altered rhyodacite and/or rhyolite porphyries. In places, large graphite clots give a bluish color to the porphyries (Fig. 2G).

The gold in the main Donlin Creek resource occurs almost exclusively as a refractory phase within arsenopyrite. Fine-grained arsenopyrite ($<20\ \mu\text{m}$) averages 40 ppm Au, whereas coarser grained arsenopyrite ($>50\ \mu\text{m}$) has a mean value of 15 ppm Au; pyrite grains typically contain 0.1 to 1.0 ppm Au and are not an important component of the overall gold resource at Donlin Creek (Placer Dome Inc., unpub. company report). Very rare visible gold has been noted in core samples from the Far Side prospect (Stan Dodd, oral commun., 1997). The veins defining the gold resource have a very consistent Ag-Au-Hg-Sb geochemical signature. Bundtzen and Miller (1997) note that 24 mineralized samples from the deposit averaged 3.2 ppm Au, 2.7 ppm Ag, 2.38 ppm Hg, 664 ppm As, and 3,500 ppm Sb. More than 2,800 samples containing >2 ppm Au were described as averaging 5.67 ppm Au, 1.89 ppm Ag, 4,369 ppm As, 140 ppm Sb, and 3.76 ppm Hg (Ebert et al., 2000a). Copper and lead concentrations are in the tens of parts per million, and zinc ranges between 100 and 200 ppm for samples from most prospects. Data from the above studies, as well as unpublished company data, indicate that, in contrast to many intrusion-related gold deposits (e.g., Thompson et al., 1999; Lang and Baker, 2001), the Donlin Creek ores are not anomalous in Bi, Te, or W.

Hydrothermal alteration is well developed where the ore zones are hosted in igneous rocks. Sericitization (fine-grained muscovite + illite) of porphyries is the most obvious alteration feature, although where the rare mafic dikes are mineralized fuchsite becomes the dominant mica, and hydrothermal biotite is present in altered porphyries at the Dome prospect. Carbonatization (Fig. 2H) and sulfidation of host rocks are typical, and where this includes disseminated arsenopyrite, the altered rock adjacent to the gold-bearing veins is also auriferous. Locally, hydrothermal kaolinite (Fig. 2H) and chlorite and/or smectite may be abundant within the sericitically and clay-altered wall rock. In contrast to the igneous rocks, there is little visible alteration of the mineralized sedimentary rocks.

Timing of mineralization has been broadly constrained by $^{40}\text{Ar}/^{39}\text{Ar}$ dating of the hydrothermal sericite. Gray et al. (1997) reported an age of 69.5 ± 1.1 Ma for the gold-forming event at the Snow prospect. Szumigala et al. (2000) indicated numerous dates on sericite of between 73.6 ± 0.6 and 67.8 ± 0.3 Ma at the Queen and Lewis prospects. These ages suggest

the gold deposition occurred within a few million years of emplacement of the ca. 75 to 69 Ma dikes and sills at Donlin Creek. Present data do not allow us to discriminate whether magmatism and gold-depositing hydrothermal activity were essentially coeval (e.g., within a few hundred thousand years of each other) or temporally distinct (e.g., separated by about 2–3 m.y.).

Mineralization at the Dome prospect

Base metal sulfide minerals are uncommon within the Donlin Creek deposit, except in the vicinity of the Dome prospect where disseminated chalcopyrite and stockworks of chalcopyrite-bearing quartz veinlets are recognized in both the porphyries and hornfels. Although not a contributor to the present Donlin Creek deposit resource, the Dome prospect commonly contains disseminated arsenopyrite and associated anomalous gold, at least some of which represents overprinting of the copper-depositing hydrothermal event by the younger Donlin Creek main-stage mineralization. However, scanning electron microscopy reveals that some of the gold at Dome occurs as grains of electrum, 5 to $40\ \mu\text{m}$ in size, and is closely associated with native bismuth and bismuth-bearing tellurides and selenides.

The geochronologic data contradict the field observations at Dome. Whereas the crosscutting relationships indicate Dome mineralization predates deposition of the main Donlin Creek gold resource, previous absolute dating does not confirm this observation. Determined $^{40}\text{Ar}/^{39}\text{Ar}$ dates of Szumigala et al. (2000) for sericite from the Dome veins are 68.0 ± 1.0 and 65.1 ± 0.9 Ma, which are younger than their argon dates on the sericite from the main gold resource. These dates are, however, in general agreement with our 66.5 Ma U-Pb date for the exposed dike from the Dome trench. We interpret these data to suggest that some granite porphyry magmatism continued until at least 66.5 Ma on the northern boundary of the Donlin Creek deposit and that this youngest magmatism may have led to argon loss and a resetting of the paragenetically earliest (i.e., ca. ≥ 74 –68 Ma) hydrothermal micas at Dome. The hornfels event at Dome must, therefore, be at least as old as this ≥ 74 to 68 Ma initial hydrothermal activity.

Fluid Inclusion Investigations

Previous studies

A reconnaissance fluid inclusion investigation was conducted on the Donlin Creek veins during initial exploration activities (Dunne, 1993). Four samples were examined from the Lewis and Far Side prospects. Dunne (1993, p. 2) noted that the fluid inclusions were “generally <2 to 3 microns which make them unsuitable for microthermometric work.” The few two-phase inclusions that she was able to measure were characterized by homogenization temperatures of 150° to 220°C . Crushing studies of the veins did indicate the presence of CO_2 in excess of 0.1 mol percent. In addition to these inclusions that seemed to be most characteristic of the gold- and sulfide mineral-bearing quartz, examination of earlier plumose-textured quartz caught up in the veins, and believed by Dunne (1993) to be recrystallized, was also carried out. Fluid inclusions in this quartz had homogenization temperatures of 210° to 260°C and contained multiple solid daughter phases.

A second internal company reconnaissance study is described by Szumigala et al. (2000). Secondary fluid inclusions were examined from igneous quartz phenocrysts in altered intrusive rocks at the Rochelieu, Queen, South Lewis, Lewis, and Dome prospects. Microscopic examination of the inclusions from the first four of these prospects, interpreted to be gold related, led to the conclusion that they were trapped at about 275° to 300°C and were dilute. In contrast, inclusions from Dome were estimated to have been trapped at temperatures in excess of 400° to 450°C, were hypersaline, and were interpreted to have been trapped close to their magmatic source.

Present study

We selected 20 quartz vein samples from drill cores for the fluid inclusion measurements. Sample selection was biased to quartz containing an abundance of ore-related sulfide minerals and/or high gold grades. These samples represent the Queen, Lewis, South Lewis, Far Side, and Dome prospects. The thin veins, which cut and often brecciate host rhyodacite dikes, appear to represent a series of tensional open-space fillings, with stibnite-realgar-orpiment assemblages occurring along the latest fractures. As was also noted by Dunne (1993), many inclusions in all sampled veins were no larger than 2 to 3 μm in maximum dimension and thus microthermometric measurements were not possible in many of the examined sections. However, we were able to obtain data from about half of these collected samples where slightly larger inclusions (typically 3–5, but sometimes as large 10 μm) were observed.

A Linkam heating and cooling stage was used for the microthermometric measurements of the fluid inclusions. In addition, laser Raman spectroscopy was performed on vapor phases in select inclusions in the petroleum geochemistry laboratory, U.S. Geological Survey, Reston, Virginia, using a Jobin-Yvon Labram HR Raman microprobe. The incident laser wavelength was 532 nm, and minimum detection limits were 0.01 mol percent for N_2 and CO_2 , and 0.03 mol percent for CH_4 and H_2S . A few yellowish inclusions were also analyzed with a Dilor SuperLABRAM Raman microprobe at the laboratory of Geoscience Australia in Canberra at a wavelength of 514.5 nm. Reconnaissance gas-liquid chromatography at the U.S. Geological Survey in Denver was performed on samples from the Lewis and Dome prospects.

Inclusions have been generally classified on the basis of phases present at room temperature and phase changes during heating and cooling. The determination of inclusion paragenesis was regimented by the classification of primary, pseudosecondary, and secondary as outlined by Roedder (1984). No inclusion could be absolutely classified as primary. Inclusions interpreted as pseudosecondary were observed in trails within individual quartz grains or as independent solitary inclusions or clusters within the quartz grains. Irregular and necked inclusions were avoided. Where a cluster of inclusions all had approximately the same microthermometric measurements, we recorded only one value for each studied parameter; in other words, recorded measurements are for fluid inclusion assemblages, a group of spatially related inclusions with identical liquid/vapor ratios and temperatures of phase changes (e.g., Goldstein and Reynolds, 1994). Trails of secondary inclusions clearly cut quartz grain boundaries in some studied sections.

Microthermometric and Raman results

Relatively consistent fluid inclusion measurements characterized ore-bearing veins from the Lewis, South Lewis, and Queen prospects (Table 2). The use of a 100 \times lens allowed clear identification of a carbonic fluid phase in many inclusions from all veins. Measured inclusions were typically about 3 to 5 μm in diameter. They are best classified as vapor poor (type 1a) and vapor rich (type 1b in South Lewis only) aqueous-carbonic inclusions, and two-phase aqueous (type 2) inclusions; the type 1 inclusions were typically present as isolated pseudosecondary inclusions or clusters of inclusions, whereas the type 2 inclusions were commonly in secondary trails. The type 1 inclusions from South Lewis samples may be part of a continuum of homogeneously trapped fluids that have a volume percent vapor of approximately 10 to 30 percent in type 1a inclusions and 50 to 75 percent in type 1b inclusions (Fig. 8A-B). Despite the broad range in vapor/liquid ratio in some vein samples, definitive evidence for fluid immiscibility is not readily observed. However, the presence of bladed carbonate in some veins, and observations on additional fluid inclusion sections by one of us (S.E.), suggests that heterogeneous trapping may have occurred at some time.

In two sections from the South Lewis prospect, some type 1 fluid inclusions were large enough (e.g., 5 μm) to allow us to clearly observe the freezing of CO_2 and subsequent melting between -59.7° and -57.1°C (Table 2). Temperatures of first melt in the type 1 inclusions were difficult to measure, but in two experiments the eutectic temperatures were unequivocally observed near -10°C , suggesting a dominance of KCl over NaCl. This potassium-rich nature to the fluids is, to a large degree, compatible with a reconnaissance bulk extraction of fluid inclusions from one gold-bearing quartz sample that was analyzed by gas-liquid chromatography. Although Na/Cl ratios are 7.4/1 for this analyzed sample from Lewis (96-199-29), a K/Cl ratio of 2.5/1 is also quite significant. It is, for example, one to two orders of magnitude greater than K/Cl ratios for intrusion-related gold deposits from eastern Alaska and Yukon (e.g., Dublin Gulch, Clear Creek, Fort Knox, Scheelite dome; all $<<1.0$; P. Emsbo, U.S. Geological Survey, unpub. data) and thus indicates the presence of relatively anomalous contents of potassium in the Donlin Creek fluids. If $\text{Na} > \text{K}$ in the late aqueous type 2 inclusions (see below) is responsible for much of the sodium in the bulk analysis, then Na/Cl for type 1 inclusions will be lower than the determined bulk ratio of 7.4/1 and the anomalous potassium could even be the dominant cation in the type 1 inclusions.

Clathrate melting was determined in type 1 inclusions from all three prospects and temperatures ranged between 7.5° and 11.0°C (Fig. 9A). The clathrate and CO_2 melting data are consistent with contamination of the CO_2 -rich vapor with methane. Although the methane prevents precise calculation of fluid salinity, the minor depression of the CO_2 -clathrate melting temperature indicates that salinities are low, perhaps no more than 3 or 4 wt percent NaCl equiv. Three-phase type 1 inclusions (e.g., water, liquid CO_2 , and vapor CO_2) were rarely seen in the South Lewis samples, but when observed, the CO_2 phases homogenized to a liquid between 15° and 24°C . Final homogenization temperatures from all the

TABLE 2. Measurements for Type 1 Fluid Inclusions from the Lewis, South Lewis, and Queen Prospects, Donlin Creek Gold Deposit

Sample no.	Prospect	No. of inclusions in FIA	Inclusion type	T _{m(CO₂)}	T _e	T _{m(ice)}	T _{m(clath)}	T _{h(CO₂)(l-v)}	T _h	Vol % CO ₂	Vol % CO ₂ vapor in CO ₂ phase
96-19-274.9	Lewis	3	1a			-3.5	10.2		229	25	
96-19-274.9	Lewis	2	1a			-3.3	10.3		230	10	
96-19-274.9	Lewis	2	1a			-3.2	10.3		237	20	
96-19-274.9	Lewis	2	1a			-3.9	10.6		245	20	
96-220-256.2	Queen	1	1a			-2.6	11.0		202	10	
96-220-256.2	Queen	1	1a			-2.9	9.7		217	10	
96-220-256.2	Queen	1	1a			-2.4			239	20	
96-220-256.2	Queen	1	1a						299	20	
96-220-256.2	Queen	1	1a				11.4		322	30	
98-490-198.7	South Lewis	2	1a			-3.9	10.3		231	15	
98-490-198.7	South Lewis	4	1a			-4.1			243	20	
98-456-220.5	South Lewis	5	1a			-3.1	7.9		250	20	
98-456-220.5	South Lewis	2	1a			-2.8	7.5		256	20	
98-490-198.7	South Lewis	2	1a				10.4		295	20	
98-490-198.7	South Lewis	4	1a		-10.3		10.5		295	25	
98-490-198.7	South Lewis	4	1a	-57.1	-10.4	-4.0	9.2		298	30	
98-490-198.7	South Lewis	3	1a			-4.1	9.4		317	25	
98-456-220.5	South Lewis	2	1a	-57.5			9.5	24.0	317	25	60
98-456-220.5	South Lewis	2	1a			-3.7	9.4		317	20	
98-456-220.5	South Lewis	3	1a			-2.6	9.1		326	30	
98-456-220.5	South Lewis	2	1a			-3.0	9.2		328	20	
98-490-198.7	South Lewis	3	1a	-57.6			9.3		337	30	
98-456-220.5	South Lewis	1	1b	-57.6			9.4		304	75	
98-456-220.5	South Lewis	1	1b	-57.5			9.3		309	70	
98-490-198.7	South Lewis	3	1b	-58.0			9.6	19.1	335	50	60
98-490-198.7	South Lewis	2	1b	-59.7				15.0	345 ¹	70	60
98-490-198.7	South Lewis	1	1b	-59.3				15.0	345 ¹	70	60

Abbreviations: FIA = fluid inclusion assemblage, T_{m(CO₂)} = CO₂ melting temperature, T_e = eutectic temperature, T_{m(ice)} = ice melting temperature, T_{m(clath)} = clathrate melting temperature, T_{h(CO₂)(l-v)} = homogenization temperature of CO₂, T_h = homogenization temperature

¹ Complete decrepitation of the inclusion occurred at this temperature

prospects ranged between 229° and 337°C for type 1a inclusions and 304° to 345°C for type 1b inclusions (Fig. 9B).

In some of the samples from South Lewis, there are also clusters of monophasic, rounded, yellowish inclusions termed type 1c. These show no changes upon cooling or heating, and may contain solid sphalerite, as suggested by laser Raman spectroscopy peaks measured at 227 and 344 to 345 (e.g., Mernagh and Trudu, 1993). However, the rare occurrence of sphalerite in polished sections of the ores and the presence of realgar in the corresponding polished section from South Lewis, suggest that this phase is more likely realgar.

To further define the composition of the type 1 inclusions, laser Raman spectroscopy was performed on the gas phase of eight inclusions in mineralized quartz from the South Lewis prospect (drill holes 98-456 and 98-490). Resulting spectra showed significant peaks only for CO₂ and CH₄. Calculated molar fractions for the vapor in these inclusions were between 81 and 94 mol percent CO₂ and 6 and 19 mol percent CH₄.

Type 2 inclusions are trails of aqueous inclusions that were clearly trapped subsequent to the type 1 inclusions. These very low salinity aqueous inclusions (Fig. 8C) are characterized by ice melting between -2.9° and -0.1°C and final homogenization temperatures of 105° to 222°C. It remains uncertain as to whether these later aqueous fluids were responsible for the late stibnite-rich mineralization. The low temperature typical of such assemblages would favor this suggestion, but, in polished section, some of the stibnite appears to be coeval with some arsenopyrite.

Estimations of ore fluid PTX

Fluid compositions were calculated for numerous type 1 inclusions in quartz from the Queen, Lewis, and South Lewis prospects, using the FLINCOR program of Brown (1989). Results suggest 92.6 to 96.6 mol percent H₂O, 3.1 to 7.2 mol percent CO₂, and 0.2 to 0.3 mol percent NaCl + KCl. Because these calculations ignore the presence of minor methane confirmed by the Raman analyses, actual fluid salinities, however, could easily be as great as 1 to 2 mol percent NaCl + KCl. These data are somewhat consistent with those recently presented by Ebert et al. (2003a), based on crushing experiments, that estimated a significant CO₂ range of 2.2 to 6.7 wt percent (or about 5–15 mol % CO₂) for these type 1 inclusions (L1 and LII types of Ebert et al.).

Average homogenization temperatures of approximately 275° to 300°C are selected as representative of minimum trapping temperatures for the fluids that deposited the gold-rich arsenopyrite. The spread in the temperature data for the inclusions suggests that some of the ore-forming fluids may have been as much as 40°C hotter or cooler. Ore-related minerals such as realgar, orpiment, cinnabar, and stibnite, which commonly appear to postdate the auriferous arsenopyrite, could have formed from these temperatures down to as low as 150° to 200°C. It remains uncertain as to whether the late type 2 aqueous inclusions are fluids from the later metalliferous episode. Commonly realgar and orpiment form at lower temperatures than arsenopyrite, but significant CO₂ within

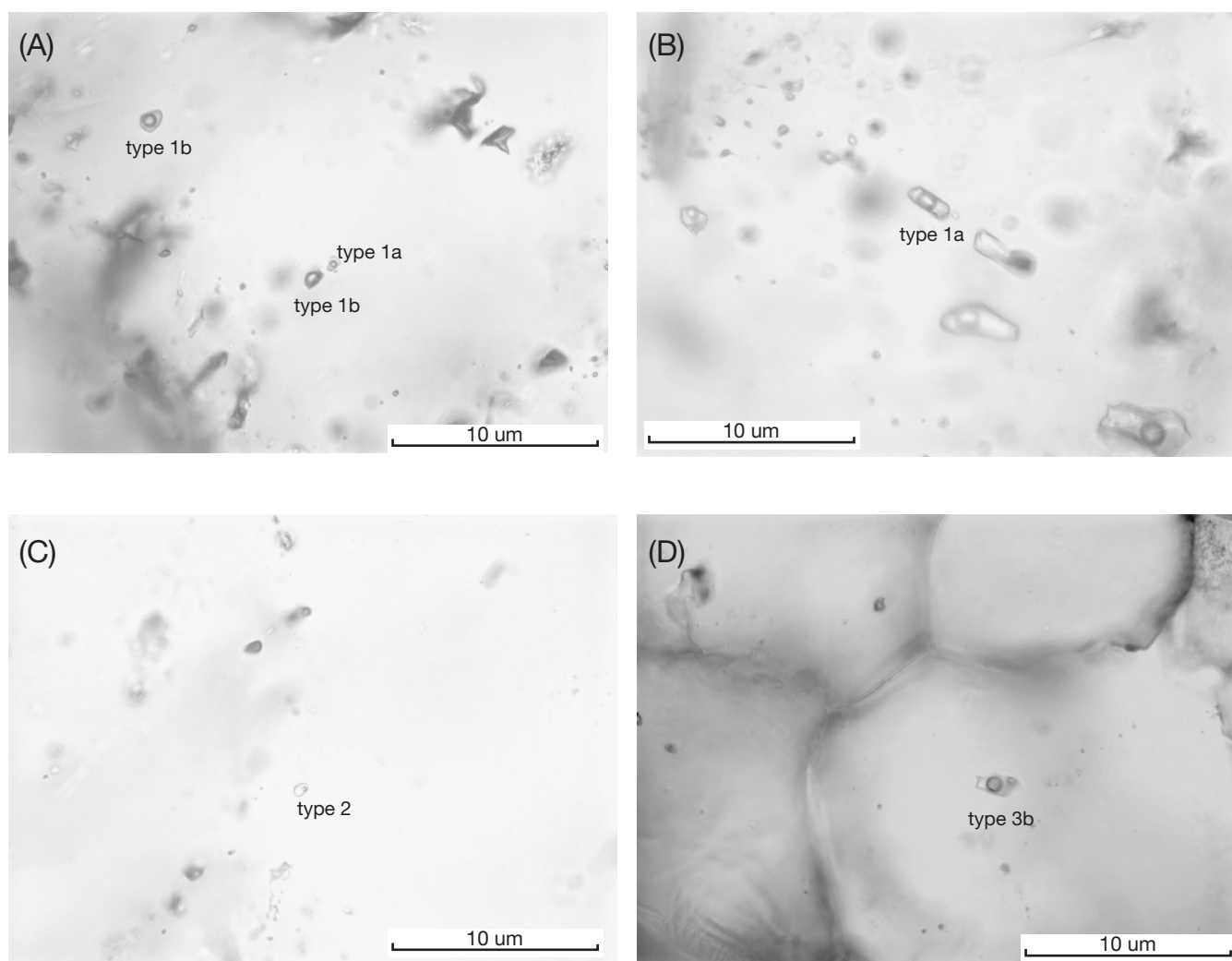


FIG. 8. Photomicrographs of fluid inclusions in quartz from the Donlin Creek gold deposit. A. Type 1a (vapor-poor) and type 1b (vapor-rich) carbonic-aqueous inclusions from the SE Lewis prospect. B. Type 1a vapor-poor carbonic-aqueous inclusions from the Queen prospect. C. Low-temperature aqueous type 1c inclusion from the SE Lewis prospect. D. Saline carbonic-aqueous inclusion, type 3b, from the Dome prospect.

the hydrothermal fluids, such as at the Donlin Creek deposit, can lower arsenic solubility and lead to higher temperature deposition of all arsenic sulfide phases (e.g., Pokrovski et al., 1996, 2002).

Trapping pressures for the ore-forming fluids within the type 1 inclusions can be estimated from published phase equilibria. The solvi from Gehrig et al. (1980) for 4.0 and 6.7 mol percent CO_2 within the $\text{H}_2\text{O}-\text{CO}_2-\text{NaCl}$ system are appropriate. If we assume the presence of minor, but some (e.g., <2 mol % NaCl + KCl) salt, and that fluid entrapment was in a mainly homogeneous field, then trapping conditions must be above the two appropriate solvi and would give minimum pressures of about 300 and 600 bars at 275° to 300°C. If trapping temperatures were greater than these homogenization temperatures, then pressures would lie at greater values along the appropriate isochores; however, trapping on the solvus is reasonable given the above mentioned presence of bladed carbonate and occasional $\text{H}_2\text{O}-\text{CO}_2$ unmixing. Assuming

lithostatic conditions, the Donlin Creek deposit formed at paleodepths of approximately 1 to 2 km.

Fluid inclusions from the Dome prospect

The metalliferous veinlets at the Dome prospect are characterized by a different assemblage of fluid inclusions. In addition to late, low-temperature type 2 aqueous inclusions, paragenetically earlier type 3a vapor-rich and type 3b hyper-saline, liquid-rich aqueous-carbonic inclusions are both abundant (Fig. 8D). The laser Raman spectroscopy analysis of one vapor bubble in a type 3b inclusion indicated equal amounts of CO_2 and CH_4 . Many areas of coexisting type 3a and 3b inclusions suggest at least episodic immiscibility. At least 50 percent of the inclusions in a number of sections are daughter phase-bearing type 3b inclusions, which may contain one or two opaque phases and/or one to three other daughter minerals. Some of the small opaque daughters are presumably sulfide minerals (chalcopyrite?), whereas the larger

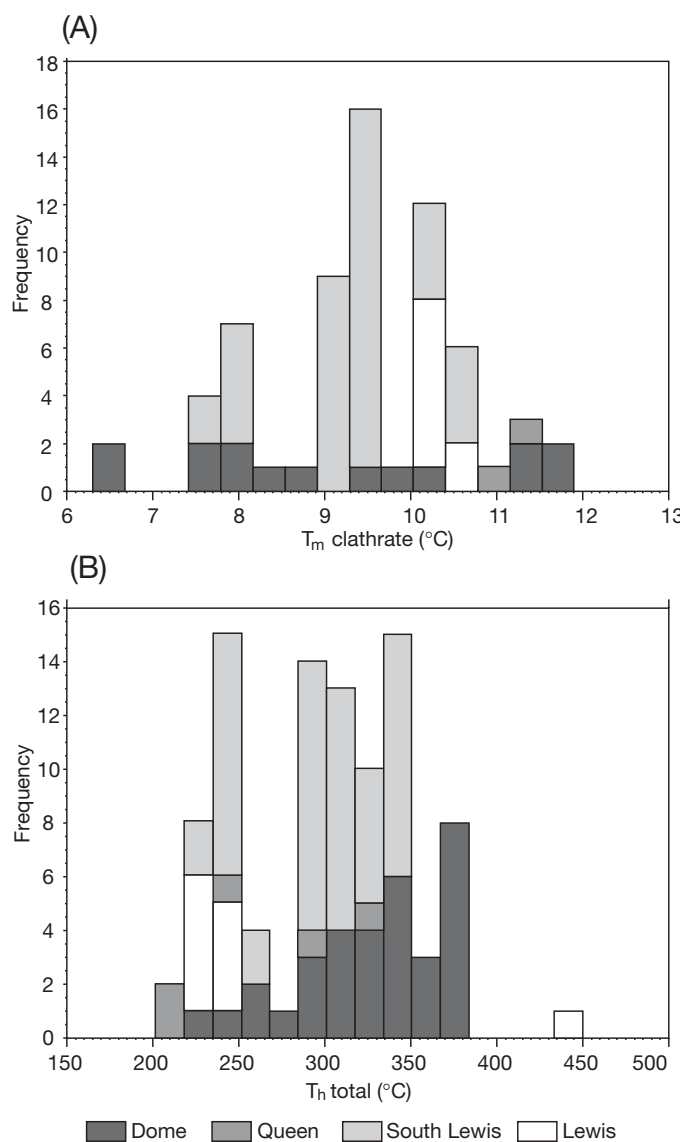


FIG. 9. Summary of microthermometric data for (A) clathrate melting and (B) total homogenization from types 1 and 3 fluid inclusions from the Queen, South Lewis, Lewis, and Dome prospects, Donlin Creek gold deposit.

phases commonly include a large halite cube and sometimes sylvite. A roundish daughter phase, recognized in two studied inclusions, was determined by laser Raman spectroscopy to be iron-rich pyrosmalite (e.g., $[\text{Fe}, \text{Mn}] \text{Si}_6\text{O}_{15} [\text{OH}, \text{Cl}]_{10}$).

The vapor-rich type 3a inclusions homogenize over a broad range of 235° to 450°C (Fig. 8B) and, similar to the type 1 inclusions within the Donlin Creek gold resource, these from Dome have clathrate melting temperatures of 7.5° to 11.4°C (Fig. 9A). Thus, the type 3a inclusions contain no more than 1 to 2 wt percent NaCl equiv. But, in contrast to type 1 inclusions from the other prospects, relatively low eutectic temperatures of -49° to -32°C were measured for both the type 3a and 3b inclusions at Dome (Table 3). This suggests that the fluids in the inclusions, and many daughter minerals themselves, may contain abundant bivalent cations. Results from

gas-liquid chromatography on a sample from Dome (96-250-160.8) indicate exceptionally anomalous K/Cl (3.4/1) and Mg/Cl (0.4/1) ratios, consistent with potassium- and magnesium-rich species. Type 3b inclusions are characterized by homogenization temperatures of 265° to 365°C and dissolution of solid phases from 275° to 390°C (Fig. 9B); final homogenization to a liquid or by solid dissolution varies with inclusion. When homogenization is by dissolution of a halite cube, estimated salinities range between 36 and 46 wt percent NaCl equiv.

In summary, relative to the veins within the main gold resource at Donlin Creek, metal-bearing veins at the Dome prospect formed from an overall more saline fluid, which had higher concentrations of magnesium and at temperatures that were as much as 100°C hotter. Furthermore, phase separation was much more commonplace in the earlier hydrothermal system at Dome.

Stable Isotope Studies

Sulfur

Sulfur isotope ratios were determined for about 50 sulfide mineral separates from gold-bearing veins in drill core from the different prospects (Table 4). All sulfur is relatively depleted in ^{34}S , with $\delta^{34}\text{S}$ values mainly ranging between -27.2 and -7.3 per mil (Fig. 10). Most values are between about -16 and -8 per mil for all prospects, including Dome. However, there is a smaller group with even more depleted sulfur values, which includes three samples of the paragenetically late stibnite from prospects in the southern part of the Donlin Creek deposit. Although petrographic observations suggest that sphalerite and much of the pyrite are essentially coeval,

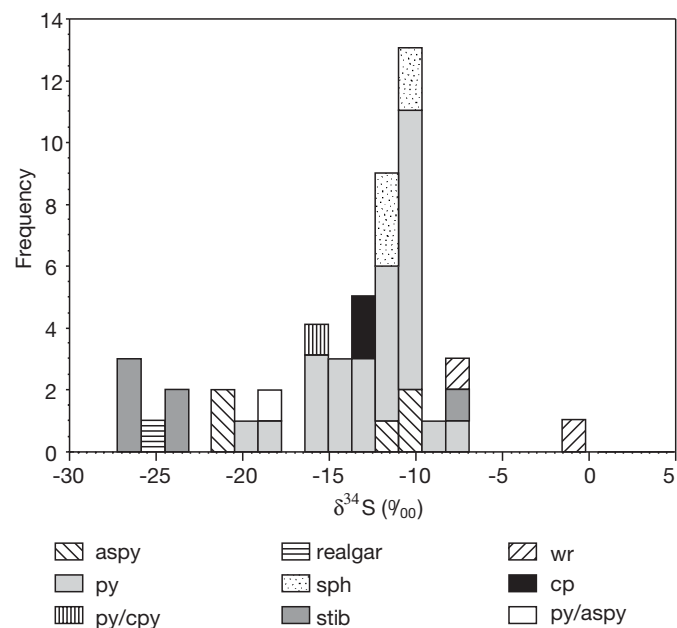


FIG. 10. Sulfur isotope data for sulfide minerals separated from mineralized zones at the Donlin Creek gold deposits and for samples of the country-rock flysch. Measurements were made on arsenopyrite (aspy), pyrite (py), mixed pyrite and chalcopyrite (py/cpy), realgar, sphalerite (sph), stibnite (stib), chalcocite (cp), mixed pyrite and arsenopyrite (py/aspy), and whole-rock samples (wr).

TABLE 3. Measurements for Type 3 Fluid Inclusions from the Dome Prospect, Donlin Creek

Sample no. ¹	Inclusion type	T _m (CO ₂)	T _m (ice)	T _m (clath)	T _e	T _m (salt)	T _m (salt 2)	T _h (vapor to liquid)	Vapor phase (% vol)	Sample no. ¹	Inclusion type	T _m (CO ₂)	T _m (ice)	T _m (clath)	T _e	T _m (salt)	T _m (salt 2)	T _h (vapor to liquid)	Vapor phase (% vol)				
96-250-120	3b		-3.5						20		3b								263	-			
	3b			8.5					10		3b								376	-			
	3b			9.3					10		3b								303	-			
	3b			7.6					-		3b								280	-			
	3b			7.5					-		3b								306	335	259	-	
	3b					275		285	-		3b								374		279	10	
	3b					310		345	-		3b								330		365	10	
	3b							225-245	-		3b								333		450 ²	10	
	3b					320	355	235-260	-		3b								313		328	20	
	3b					330		255	-		3b								190		310	15	
	3a							355 ³	40		3b								278		238	10	
	3a							450 ²	40		3b								287		277	7.5	
	3b		8.0			350		295	2		3b								318		258	7.5	
	3b					333	355	325	2		3b			3.7	-14						338	20	
	3a							400	40		3b										337	15	
	3a							355-360	30-50		3b										293	7.5	
	3a							380 ³	40		3b								290 ²		320	10	
	3b							376 ³	-	96-250-120	3a										406 ³	50	
	3b					390 ²		308	-		3b										430 ²	20	
	3b					330	352	275	-		3a										3503	45	
	3b						310	348 ³	-		3b										245	10	
	3b							370 ³	-		3b										257	10	
	3b					350		265	-		3b										258	10	
	3a			9.3					50		3b			5.8							277	30	
	3a			4.0					50														
	3a			9.0					50														
	3a							400-450 ³	50	96-250-186	3b												
	3a							375 ³	50		3b												
	3a								50		3b	-59.0		11.4									
	3a			3.7					50		3b	-70.0		11.3									
	3a			9.4					50		3b												
	3a			8.7					50		3b												
	3b		-6.3						321		3b												
	3a			6.6					50		3b												
	3a			6.2					50		3b												
	3a			7.6					50		3b												
	3a			14.4					50	D1	3b		-26.9		-45							287	10
	3a			7.7					50		3b												
	3a							362	40		3a			11.9									
	3b		-3.1		-4			228	10		3b												
	3b		-4.3		-20			251	7.5		3a												
	3b							263	10		3a												
	3b							265	-		3b												
	3b					285		265	-		3b												
	3b					-15	400 ²	365	-		3a												
	3b						462 ²	321	-		3a												
	3b						400 ²	393	-		3a												
	3b					-21	415 ²	415 ²	20		3a												
	3b							329	10		3b												
	3b						252	>430	-		3b												
	3b						255	374	10		3a												
	3b						400 ²	314	10		3b												
	3b							334	10														

Abbreviations: T_h = homogenization temperature, T_m(CO₂) = CO₂ melting temperature, T_m(ice) = ice melting temperature, T_m(clath) = clathrate melting temperature, T_m(salt) = salt dissolution temperature, T_m(salt 2) = dissolution temperature for 2nd salt, - = no measurement

¹ Sample numbers refer to studied drill core

² Complete decrepitation of the inclusion occurred at this temperature

³ Homogenization to vapor

the extremely variable temperature estimates from the pairs in Table 4 suggest significant disequilibrium between various sulfide minerals.

The δ³⁴S values for the Donlin Creek deposit are notably lower than most published data for orogenic (e.g., Kerrich,

1989), epithermal (e.g., Field and Fifarek, 1985), and Carlin-type (e.g., Hofstra and Cline, 2000) gold deposits. Nevertheless, such data may be interpreted as reasonable for ore-related sulfur derivation from the sedimentary rocks of the Kuskokwim basin. At low temperature, synsedimentary

TABLE 4. Sulfur Isotope Analyses of Samples from and Adjacent to Gold-Bearing Veinlets, Donlin Creek Deposit and Surrounding Region

Sample no.	Prospect/area	$\delta^{34}\text{S}$ (‰)	Mineral	Comments (gold grades, host rocks, etc.)
Ore-related sulfides				
96-37-trench	Lewis	-10.9	Pyrite	0.2 g/t Au; rhyodacite porphyry with carbonaceous blebs
96-195-251	Lewis	-26.9	Stibnite	17.1 g/t Au; mafic dike
96-195-274.9	Lewis	-7.8	Pyrite	10.3 g/t Au; >15% arsenopyrite + stibnite; fine-grained rhyodacite
96-195-274.9	Lewis	-26.2	Stibnite	
96-220-215.5	Queen	-14.7	Pyrite	
96-220-215.5	Queen	-11.2	Sphalerite	
96-220-256.2	Queen	-11.6	Arsenopyrite	135 g/t Au, 4.9% As, 3.6 % Zn; also anomalous Ag, Bi, Cu, Hg, Mn, Pb, Sb, W; rhyodacite-mafic dike contact
96-220-256.2	Queen	-12.4	Chalcopyrite	
96-220-256.2	Queen	-11.3	Pyrite	
96-220-256.2	Queen	-10.8	Sphalerite	
96-220-256.2	Queen	-24.2	Stibnite	
96-233-271	Lewis	-11.8	Pyrite	Massive pyrite with only 0.2 g/t Au; siltstone
96-247-186.8	Queen	-14.2	Pyrite	2.37 g/t Au; fine-grained rhyodacite
96-247-225.2	Queen	-20.5	Arsenopyrite	14.5 g/t Au; siltstone-rhyodacite contact
96-247-225.2	Queen	-13.5	Pyrite	
96-247-307.5	Queen	-18.1	Pyrite/arsenopyrite	Sheared mafic dike with 10 g/t Au
96-250-82	Dome	-10.0	Arsenopyrite	1.15 g/t Au; biotite hornfels
96-250-120	Dome	-10.0	Pyrite	1.36 g/t Au; biotite hornfels
96-250-159.8	Dome	-10.7	Pyrite	
96-250-160.8	Dome	-15.7	Pyrite/chalcopyrite	
96-250-160.8	Dome	-11.2	Sphalerite	
96-250-186	Dome	-12.6	Chalcopyrite	
96-250-186	Dome	-10.5	Pyrite	
96-250-186	Dome	-11.1	Sphalerite	
96-250-187	Dome	-13.1	Pyrite	
96-250-187	Dome	-10.8	Sphalerite	
96-254-35.8	Far Side	-11.9	Pyrite	
96-255-122.5	Far Side	-14.1	Pyrite	
97-387-382.5	Duqum	-10.6	Pyrite	Quartz monzonite
97-392-189.3	Dome	-9.8	Pyrite	24.5 g/t Au, with anomalous As-Cu-Bi-Mo-W; fine-grained rhyodacite that is altered to biotite hornfels
97-398-157.3	Vortex	-16.4	Pyrite	Fine-grained rhyodacite
97-448-65.5	South Lewis	-12.4	Pyrite	Rhyodacite; chalcopyrite, covellite, and chalcocite are present; 1.48 g/t Au
97-478-262.4	Lewis	-9.9	Pyrite	
98-449-199	Acma	-18.8	Pyrite	Orpiment and native arsenic also present; veinlet in rhyodacite
98-449-199	Acma	-21.2	Arsenopyrite	
98-453-36.1	Lewis	-15.8	Pyrite	1 g/t Au; veinlet is highly brecciated; along shale-fine-grained rhyodacite contact
98-453-36.1	Lewis	-10.0	Arsenopyrite	
98-455-220.5	South Lewis	-27.2	Stibnite	9.57 g/t Au in realgar-rich veinlet along rhyodacite-graywacke contact
98-455-220.5	South Lewis	-24.6	Realgar	
98-456-270.06	Lewis	-10.5	Pyrite	Stibnite-realgar breccia fragments in quartz-carbonate vein in mafic dike; 2.3 g/t Au
98-456-270.06	Lewis	-23.8	Stibnite	
98-478-32	Lewis	-20.2	Pyrite	Aphanitic-rhyodacite porphyry contact
98-489-210	South Lewis	-9.0	Pyrite	Rhyodacite
98-489-297.26	South Lewis	-7.3	Stibnite	Massive stibnite in flysch
98-489-297.26	South Lewis	-15.8	Pyrite	0-2 cm into flysch wall rock adjacent to massive stibnite
98-489-297.26	South Lewis	-12.0	Pyrite	2-6 cm into flysch wall rock adjacent to massive stibnite
98-490-198.7	South Lewis	-11.7	Pyrite	Rhyodacite; veinlet contains abundant pink carbonate
Country-rock sulfur sources				
97-478-259.1	Lewis	-15.9	Pyrite	Flysch with preore pyrite clots
97-478-259.1	Lewis	-10.1	Pyrite	Preore pyrite separate from flysch
98AM269	Ridge east of Donlin Creek	-0.2	Whole rock	Fresh graywacke of the Kuskokwim Group
98AM278B	Cliff along Kuskokwim River	-7.5	Whole rock	Fresh fine-grained sandstone of the Kuskokwim Group

sulfide that formed from reduction of seawater sulfate during deposition of the Kuskokwim Group rocks should have been about 20 to 25 per mil lighter than the sulfate or about 0 per mil and even significantly lighter if anaerobic bacteria were involved. This is consistent with whole-rock flysch and syngenetic pyrite values of -15.9 and -10.1 per mil, respectively, for country rock at the Lewis prospect (Table 4).

Coarser grained sedimentary rocks, deposited in more active parts of the basin, which thus had lesser bacterial action, show values closer to 0 per mil (e.g., sample 98AM269, Table 4). Such a difference also suggests that bacterial reduction of sulfate, and not thermochemical reduction, was the dominant cause of the light sulfur in the country rocks.

The H₂S produced by decomposition of synsedimentary pyrite will essentially have the same $\delta^{34}\text{S}$ composition as the original pyrite (e.g., Ohmoto and Rye, 1979). Therefore, sulfur in syngenetic pyrite and, to a lesser degree, in organic matter within the fine-grained material of the Kuskokwim basin is the most likely source for the sulfur in the Donlin Creek deposit. It remains uncertain how that sulfur became part of the hydrothermal system, but obvious scenarios most likely relate to a metamorphic and crustal melting episode triggered by rising mantle melts into the base of the basin (see below discussion on radiogenic isotope data). One possibility is that the sulfur was released directly into the fluid via devolatilization during metamorphism of rocks that are still at depth in the basin. Alternatively, during melting of flysch also deeper within the basin, sulfur may have entered the ca. 70 Ma melts and then was exsolved later in the magmatic history. Magmatic sulfur has traditionally been accepted to be 0 ± 5 per mil (e.g., Ohmoto and Rye, 1979); however, it is now recognized that when a magma contains a significant crustal melt component, magmatic $\delta^{34}\text{S}$ values can approximate those of the melted crust (e.g., as low as -20% in Ohmoto and Goldhaber, 1997). In summary, either metamorphic or magmatic processes are both compatible with the depleted sulfur isotopes.

The reason for the group of very depleted sulfur measurements (i.e., -18 to -27%) is also unclear. Our preferred explanation is that the sulfur data reflect two distinct hydrothermal episodes. The earlier episode, which included deposition of most of the auriferous arsenopyrite and the pyrite, was characterized by sulfur contribution from a relatively less depleted sedimentary rock source. The more negative $\delta^{34}\text{S}$ values characterize a later episode of sulfide deposition, including formation of realgar, orpiment, and most of the stibnite, with the associated fluid containing sulfur that was originally sourced in a distinctively more ^{34}S depleted part of the basin. The samples defining the more depleted population were all collected from the Queen prospect and areas to the south. This could reflect the fact that the later hydrothermal fluid flow event was more focused into this part of the Donlin Creek deposit. However, minor stibnite reported from drill cores at the Dome and Quartz prospects to the north was not sampled for the sulfur study, and it is thus not clear as to whether the second event was at least locally present in the northern part of the deposit.

Alternative explanations for the broad range in $\delta^{34}\text{S}$ values, such as variations in temperature, redox, or fluid immiscibility, are less likely. As indicated by the relationships in Ohmoto and Goldhaber (1997), a minor temperature and/or redox change within the reduced hydrothermal system at Donlin Creek, or H₂O-CO₂ immiscibility for a reduced hydrothermal system, would not have had a major effect on the sulfur isotope ratios.

Oxygen and hydrogen

The $\delta^{18}\text{O}$ data for gold- and sulfide mineral-bearing quartz are also spread over a relatively broad range between about 11 and 25 per mil (Table 5). No systematic relationships are evident between gold grade or sulfide mineralogy and $\delta^{18}\text{O}$. However, the quartz vein samples from the Dome prospect are, as a whole, ^{18}O depleted when compared to the prospects farther south at the Donlin Creek deposit. Measured $\delta^{18}\text{O}$

TABLE 5. Oxygen and Hydrogen Isotope Analyses of Hydrothermal Minerals from and Country Rocks to Gold-Bearing Veinlets, Donlin Creek Deposit

Sample no.	Prospect	$\delta^{18}\text{O}$	δD	Comments
Gold-bearing veinlets ($\delta^{18}\text{O}_{\text{qtz}}$, $\delta\text{D}_{\text{fuchsite}}$)				
96-37-trench	Lewis	14.6		
96-195-251	Lewis	24.7		
96-195-274.9	Lewis	24.6		
96-220-215.5	Queen	20.5		
96-220-256.2	Queen	22.3		
96-247-186.8	Queen	16.8		
96-247-225.2	Queen	14.8		
96-247-307.5	Queen	23.3		
96-250-120	Dome	16.2		
96-250-159.8	Dome	14.8		
96-250-160.8	Dome	11.2		
96-250-186	Dome	17.4		
96-250-187	Dome	16.9		
96-250-188	Dome	15.9		
96-254-35.8	Far Side	14.3		
96-255-122.5	Far Side	14.8		
96-255-124.1	Far Side	19.2		
98-456-270.06	Lewis		-123	Fuchsite in quartz in mafic dike
Whole-rock samples				
95-175-129.8	Vortex	15.3		Rhyodacite
96-250-129	Dome	14.2		Weakly altered quartz-feldspar porphyry
96-250-131	Dome	14.5		Altered quartz-feldspar porphyry
96-254-33.5	Dome	15.1		Unaltered rhyodacite
96-255-114	Dome	11.1		Rhyodacite
97-363-64	Dome	14.0		Rhyolite
97-385-239	Quartz	11.8		Moderately altered
97-388-221.8	Duqum	11.1		Porphyry
97-398-157.3	ACMA	16.8		Porphyritic rhyodacite
97-437-266	Nuno	13.7		Rhyodacite
98-387-382.5	Duqum	11.9		Quartz monzonite
98-478-32	Lewis	18.7		Fine-grained rhyodacite porphyry
98-478-90	Lewis	15.4		Porphyritic rhyodacite
98-489-210	South Lewis	15.0		Altered rhyodacite
99AM503	Southwest of Lewis	17.4		Barren porphyry 13 km southwest of Lewis
DT-99-265	Dome	15.0		Porphyry from trench
Mineral separates from igneous country rock				
95-175-129.8	Vortex	14.3		Quartz from rhyodacite
95-175-129.8	Vortex	2.9		Potassium feldspar from rhyodacite
97-387-382.5	Duqum	14.6	-117	Quartz and biotite from quartz monzonite
97-417-133	Rochelieu		-92	Fuchsite from altered mafic dike
98-478-90	Lewis		-81	Chlorite from rhyodacite
98-490-198.7	South Lewis	14.2		Quartz from rhyodacite

values for Dome samples never exceed 17.4 per mil, whereas more than half the samples from Queen and Lewis have values between 20 and 25 per mil.

The broad range of $\delta^{18}\text{O}$ values at Donlin Creek is identical to that characterizing epizonal mercury-antimony mineralization throughout the Kuskokwim basin (e.g., Goldfarb et al., 1990). These $\delta^{18}\text{O}$ values are generally higher than those measured for quartz from most volcanic rock-hosted

epithermal gold deposits (e.g., Field and Fifiarek, 1985). In contrast, the range in $\delta^{18}\text{O}$ for quartz in Carlin-type deposits is between about 0 and 25 per mil, which does overlap the Donlin Creek range, but also extends to much lower values. The data for Carlin ores are interpreted to be products of the mixing between meteoric water and fluids from isotopically heavier sources (e.g., magmatic or metamorphic and exchanged meteoric; Hofstra and Cline, 2000).

The fluid inclusion data indicate a wide variation in depositional temperatures over the life of the Donlin Creek ore system. A spread of 8 per mil in the measured $\delta^{18}\text{O}$ data would be consistent with quartz precipitation from a single oxygen reservoir over a temperature range of 200° to 400°C. In addition, fluid interaction with rocks of the Kuskokwim Group, which has average $\delta^{18}\text{O}$ values of 18 to 20 per mil (Gray et al., 1997), might also explain some of the higher values. We suggest that the $\delta^{18}\text{O}$ data from Donlin Creek are best explained by a combination of both variations in temperature and variable water-rock interaction. A major influx of an unexchanged, isotopically light meteoric water into the ore-forming system is unlikely because, unlike Carlin-type systems, no calculated $\delta^{18}\text{O}$ fluid values for vein quartz from any of the Donlin Creek prospects approach the meteoric water line (Fig. 11). However, oxygen data for the vein quartz do not preclude the contribution of fluids of magmatic, metamorphic, or highly exchanged meteoric origin.

A group of relatively fresh granitoid samples was collected from drill cores to determine $\delta^{18}\text{O}$ for the least altered intrusions

(Table 5). Although some of these samples may have been slightly altered, the whole-rock data cluster with $\delta^{18}\text{O}$ values between about 11 and 15 per mil. Such data are consistent with a predominant flyschoid source for the granitic rocks and the range is typical of, to even slightly heavier than, most reported S-type melts (e.g., O'Neil et al., 1977; Taylor and Sheppard, 1986). Quartz separates from some of these samples also fall within the same S-type intrusion range. However, a single K-feldspar separate from these granitoids has a $\delta^{18}\text{O}$ value of 2.9 per mil and provides compelling evidence that, at some time, unexchanged meteoric fluids were present within the Donlin Creek ore zones. The fact that such low values are not observed for any of the quartz veins, nor for the above whole-rock samples, suggests that this was a minor and/or low-temperature event during which exchange only took place with the feldspars.

Calculation of precise $\delta^{18}\text{O}$ fluid values (Fig. 11) is difficult, in large part due to the wide variation in temperatures obtained from the fluid inclusion studies. Using the quartz-water fractionation curve of Matsuhisa et al. (1979), ore fluids would be 4 per mil lower than measured quartz values at 400°C and 12 per mil lower at 200°C. Considering that the higher temperature fluid inclusion homogenization measurements were associated with the Dome prospect, we estimate that most fluid $\delta^{18}\text{O}$ values were consistently between 7 and 12 per mil over the entire deposit (assuming 400°C at the Dome prospect and 300°C for veins elsewhere at the deposit).

The $\delta^{18}\text{O}$ values measured by Szumigala et al. (2000) on nine sericite separates from the various prospects at the

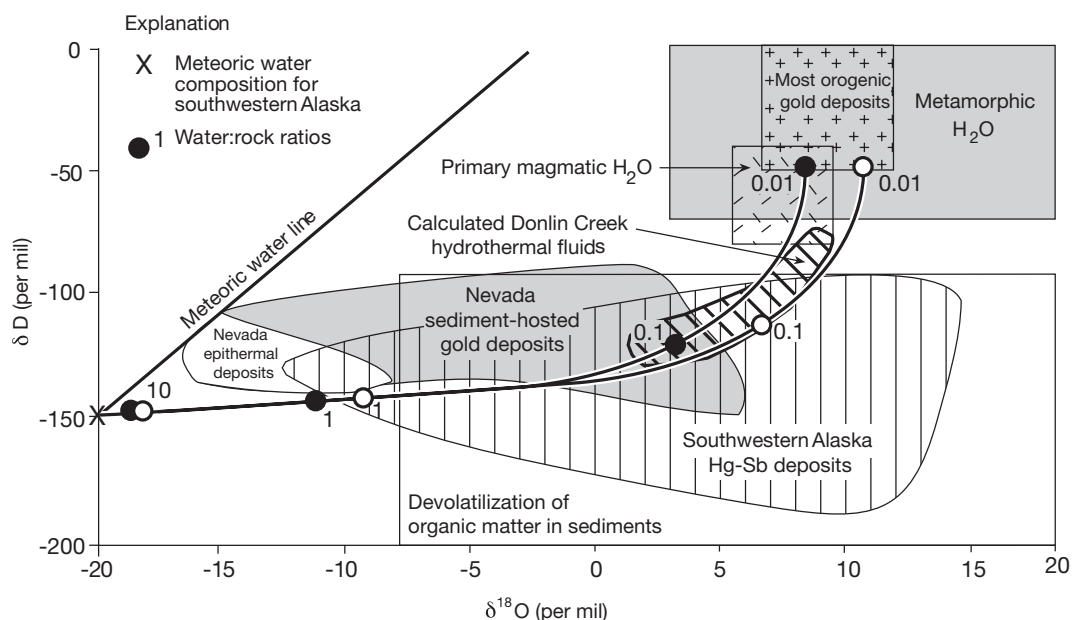


FIG. 11. Plot of δD vs. $\delta^{18}\text{O}$ for ore fluids from the Donlin Creek gold deposit, SW Alaska. Calculated fluid evolution paths at 200°C (black circles) and 300°C (open circles), which are the estimated temperatures for formation of the stibnite- and arsenopyrite-bearing veins in the gold resource area, show that extremely low water to rock ratios would be required if meteoric water was a major component in the ore fluids. (Calculations assume an initial $\delta^{18}\text{O}$ rock value of 16‰ and δD rock value of -60‰.) A crustal source is thus required for the bulk of the ore fluid, and magmatic, metamorphic and/or organic reservoirs are all permissible (see text for details). Magmatic, metamorphic, and organic (e.g., devolatilization of organic matter in sediments) water fields after Sheppard (1986); fields for Nevada epithermal and Carlin deposits after Field and Fifiarek (1985); and field for SW Alaska deposits after Gray et al. (1997).

Donlin Creek deposit ranged between 4.5 and 12.5 per mil. Calculated fluid values were reported to be between 1 and 9 per mil, assuming mineral-water fractionation at 300°C for all prospects, except for the Dome prospect where a 400°C temperature was used. Thus, although there is overlap in the calculated fluid range between our data and those of Szumigala et al. (2000), the more depleted range from sericite is particularly indicative of the influx of meteoric water into the Donlin Creek systems, as noted by Szumigala et al. (2000), although such water would have been highly exchanged at that point. Gray et al. (1997) also used oxygen isotope data to suggest some similar mixing of isotopically heavy metamorphic fluids with a lighter meteoric water in the formation of epizonal mercury-antimony deposits throughout southwestern Alaska.

Hydrogen isotope data for fuchsite and chlorite from the margins of gold-bearing veins collected during this study, as well as for the sericites studied by Szumigala et al. (2000), are all consistent with a fluid that is lighter than normal nonorganic metamorphic or magmatic sources. Measured δD values for all such micas range between about -150 and -80 per mil. Using experimentally determined equilibrium fractionation data (e.g., Kyser, 1987), and assuming crystallization temperatures of 300° to 400°C, calculated fluid δD values will be typically 20 to 30 per mil higher than these measured values (Fig. 11).

The hydrogen isotope data, with some micas forming from a fluid with δD values as low as -120 per mil, indicate some influx of either exchanged meteoric water and/or organically derived hydrogen. The oxygen data from K-feldspar and sericite are consistent with the former interpretation, although we stress that the narrow and high range of $\delta^{18}O$ values requires the meteoric fluid to be very highly exchanged. Alternatively, the abundance of organic matter in the rocks of the Kuskokwim Group would lead to a significant methane component within any fluid produced during devolatilization and melting of the flysch. Oxidation of such methane, possibly during interaction of the ore fluid with the Donlin Creek sill-dike complex, would lead to a relatively D depleted organic water measured within the hydrothermal micas (e.g., Sheppard, 1986). The observed range of about 70 per mil for the various micas suggests that either process leading to the depleted hydrogen isotope values showed significant local variation at Donlin Creek.

Radiogenic Isotope Studies

Analytical procedures

Twenty-one samples of igneous and sedimentary rocks from drill core at the Donlin Creek deposit and surface outcrops in the region were analyzed for neodymium, strontium, and/or lead isotope compositions using a multicollector, Finnigan-MAT 262 mass spectrometer at the U.S. Geological Survey, Reston, Virginia. Stibnite and pyrite from gold-rich veinlets were analyzed for lead isotopes. Long-term reproducibility of neodymium isotopes was monitored using the La Jolla standard, $^{143}\text{Nd}/^{144}\text{Nd} = 0.511845 \pm 5$ ($n = 45$); neodymium data were normalized to $^{146}\text{Nd}/^{144}\text{Nd} = 0.7219$. Total neodymium blanks were <20 pg, insignificant relative to the neodymium contents of the rocks. Depleted mantle

model ages were calculated as in the model of DePaolo (1981). Long-term reproducibility of strontium isotope analyses was monitored using SRM 987, $^{87}\text{Sr}/^{86}\text{Sr} = 0.710245 \pm 5$ ($n = 35$); total blanks were <50 pg for strontium. A total of 32 whole-rock and sulfide lead isotope measurements were obtained. Samples were leached in 1N HBr-2.5N HCl (leach) and then dissolved in HNO_3 -HCl (residue). Lead isotopes were purified using standard procedures and corrected for mass fractionation by about 0.12 percent per amu according to replicate measurements of NBS 981 ($n = 45$). Total lead blanks were less than 50 pg, insignificant relative to lead abundances in rocks and sulfide minerals.

Nd-Pb-Sr isotopes

Magmatic rocks from the Donlin Creek deposit have negative ϵ_{Nd} values (Figs. 12–13A; Table 6). Rhyodacite dikes associated with the ores at five of the prospects range in ϵ_{Nd} (at 70 Ma) from -8.7 to -3.1; a coarser granite dike at the Duquom prospect also falls in this range with ϵ_{Nd} at -5.5. Auriferous felsic hypabyssal dikes elsewhere in the Kuskokwim basin (e.g., Julian Creek, Granite Creek, Stuyahok, and Gold Run), as well as the Barometer Mountain granitic stock spatially associated with epizonal mercury mineralization, span only a slightly broader range than Donlin Creek. Least altered igneous rocks from Gold Run and Stuyahok have $\epsilon_{\text{Nd}} \sim -1$ to 0, and ϵ_{Nd} is -9.6 for dikes at Julian Creek. Hydrothermally altered dikes may have similar (e.g., Donlin Creek, Gold Run), significantly higher (e.g., Julian Creek, Granite Creek), or lower (e.g., Stuyahok) ϵ_{Nd} values compared to unaltered dike rock (Table 6). Sedimentary rocks from the

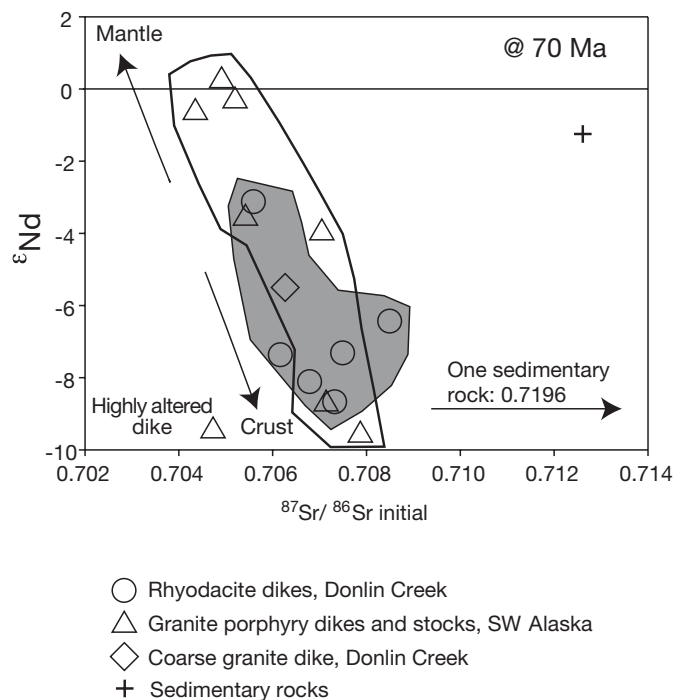


FIG. 12. Diagram showing ϵ_{Nd} values vs. $^{87}\text{Sr}/^{86}\text{Sr}$ at 70 Ma for various host and country rocks for the Donlin Creek deposit and for granite porphyry dikes elsewhere in SW Alaska. The ϵ_{Nd} values are much lower than that of the Late Cretaceous mantle and indicate variable melt contributions from continental crust.

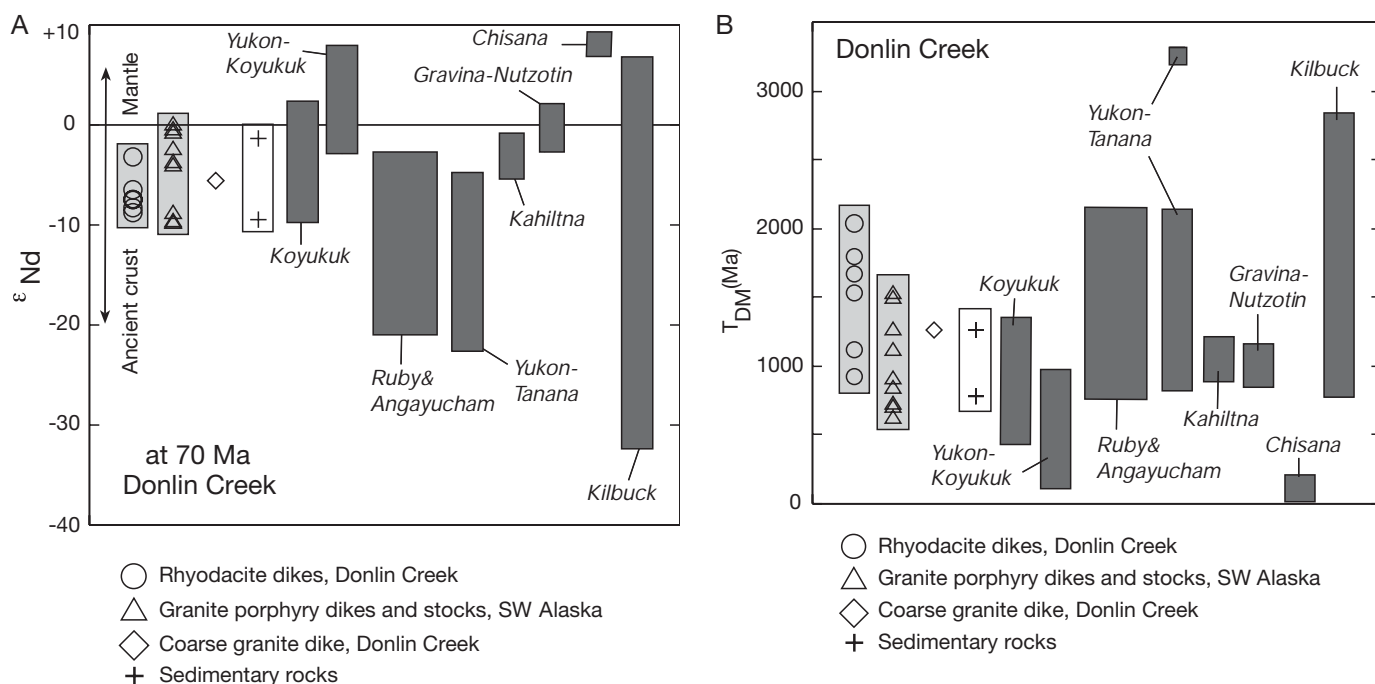


FIG. 13. Diagrams showing variations in (A) ϵ_{Nd} and (B) depleted mantle model ages (T_{dm}) for dikes at Donlin Creek and elsewhere within the Kuskokwim basin (at 70 Ma). Shown for comparison are the calculated ϵ_{Nd} and T_{dm} values for rocks from adjacent terranes in interior Alaska: Cretaceous plutons from the Ruby and Angayucham terranes (Arth et al. 1989a), Late Cretaceous and early Tertiary volcanic rocks from the Koyukuk terrane (e.g., on the northern side of Yukon-Koyukuk basin; Moll-Stalcup and Arth, 1991), Cretaceous igneous rocks from the Yukon-Koyukuk basin (e.g., the Late Cretaceous volcanic fields south of the Kaltag fault; Arth et al., 1989b), Cretaceous and Tertiary plutons from the Yukon-Tanana terrane (Aleinikoff et al., 2000), Jurassic to Cretaceous flysch of the Kahiltna and Gravina-Nutzotin belts (Aleinikoff et al., 2000) and overlying Early Cretaceous Chisana volcanic rocks (Aleinikoff et al., 2000), and Precambrian magmatic rocks from the Kilbuck terrane (Moll-Stalcup et al., 1996).

TABLE 6. Sm-Nd Isotope Data for Igneous and Sedimentary Rocks from the Donlin Creek Gold Deposit and from Elsewhere in Southwestern Alaska

	Sm (ppm)	Nd (ppm)	$^{147}\text{Sm}/^{144}\text{Nd}$	$^{143}\text{Nd}/^{144}\text{Nd}$ (measured)	Error (2σ)	ϵ_{Nd} (initial) 70 Ma	T_{dm} (Ga)	Sample description
Rhyodacite/granite porphyry dikes, Donlin Creek								
DC95-175-129.8	4.09	18.32	0.1350	0.512192	0.000008	-8.11	1.67	Fresh rhyodacite; Vortex prospect
DC97-398-157.3	3.45	13.41	0.1556	0.512287	0.000007	-6.44	2.04	Rhyodacite, aphanitic; porphyritic; ACMA prospect
DC97-437-266	6.20	29.91	0.1254	0.512159	0.000008	-8.67	1.54	Rhyodacite; Nuno prospect
DC98-478-32-2	5.74	24.09	0.1441	0.512236	0.000009	-7.33	1.80	Rhyodacite, aphanitic; porphyritic; Lewis prospect
DC98-478-90	5.24	28.20	0.1124	0.512451	0.000007	-3.13	0.93	Rhyodacite, aphanitic; porphyritic; Lewis prospect
DC98-489-210	0.03	0.18	0.1008	0.512215	0.000008	-7.36	1.13	Altered rhyodacite; South Lewis prospect
DC98-387-382.5	3.76	18.11	0.1256	0.512321	0.000008	-5.51	1.26	Granite porphyry dike, Duqum prospect
Other granite porphyry dikes and stocks, SW Alaska								
98AM-270	4.30	21.98	0.1183	0.512108	0.000008	-9.60	1.51	Granite porphyry on ridge, head of Julian Ck.
98AM-271	1.05	5.37	0.1183	0.512479	0.000009	-2.36	0.92	Rhyolitic porphyritic dike, Julian Ck. area
98AM272	2.53	12.24	0.1250	0.512155	0.000006	-8.74	1.54	Granite porphyry on ridge, head of Julian Ck.
98AM-273	4.23	20.48	0.1249	0.512398	0.000006	-4.00	1.12	Altered feldspar-quartz porphyry, Granite Ck.
98AM-274	4.42	27.50	0.0972	0.512406	0.000007	-3.60	0.85	Granite porphyry, Barometer Mtn.
98AM-275A	2.62	16.31	0.0972	0.512573	0.000008	-0.34	0.63	Fresh, Stuyahok trenches
98AM-275B	3.50	21.03	0.1006	0.512106	0.000007	-9.48	1.27	Highly altered, Stuyahok trenches
98AM-276A	6.18	31.63	0.1182	0.512611	0.000006	0.21	0.71	Altered, ridge above Gold Run
98AM-277	6.76	36.44	0.1122	0.512563	0.000005	-0.67	0.74	Fresh, coarse granite ridge above Gold Run
Sedimentary rocks								
98AM-269	3.43	18.13	0.1144	0.512534	0.000006	-1.25	0.80	Graywacke, Kuskokwim Gr., east of Donlin Ck.
98AM-278A	4.62	27.05	0.1033	0.512117	0.000005	-9.29	1.29	Shale, cliff along Kuskokwim River

Kuskokwim Group also differ widely in ϵ_{Nd} (-1.3 for graywacke and -9.3 for shale at 70 Ma). The depleted mantle model age (T_{dm}) varies from about 0.6 to 2 Ga (Fig. 13B). Magmatic rocks from Donlin Creek differ from Late Cretaceous mantle (ϵ_{Nd} typically higher than 6) and attest to contributions of continental crust. Magmatic rocks having $\epsilon_{Nd} < -5$ are likely to represent predominantly crustal melts or rocks that reacted extensively with radiogenic reservoirs during melt transport and emplacement.

Whole-rock lead isotope compositions of dikes from the Donlin Creek deposit ($n = 14$) display a wide range (Table 7). Present-day $^{206}Pb/^{204}Pb$ varies from 18.760 to 19.306, $^{207}Pb/^{204}Pb$ from 15.554 to 15.616, and $^{208}Pb/^{204}Pb$ from 38.364 to 38.817. Some residues are relatively more radiogenic than the leaches, implying involvement of different fluids and melts. Age-corrected compositions (at 70 Ma) are shown in Figure 14A-B. As was the case for neodymium, lead isotope compositions of felsic granitic dikes at Donlin Creek and from elsewhere in the Kuskokwim basin are indistinguishable as separate groups. Lead isotope compositions of sulfide minerals are also indistinguishable from the dikes. Although lead data for ten sedimentary rocks partly overlap the compositions of the magmatic rocks and sulfide minerals, they are generally more radiogenic (Table 7). The Kuskokwim basin dikes plot below the average crustal lead evolution curve ($\mu = 9.74$, Stacey and Kramers, 1975; Fig. 14A).

The dikes from the Donlin Creek deposit have a range of $^{87}Sr/^{86}Sr$ (at 70 Ma) ratios from about 0.70559 to 0.70850 (Table 8). For the most part, this range overlaps other

mineralized dikes in the Kuskokwim region (Fig. 12). However, excluding one highly altered sample, granite dikes at Stuyahok and Gold Run clearly differ from dikes at Donlin Creek and elsewhere by their initial $^{87}Sr/^{86}Sr$ of about 0.70521. This, coupled with their previously described higher ϵ_{Nd} values at 70 Ma, indicates some mantle contribution to the felsic dikes in more peripheral parts of the Kuskokwim basin.

Implications of the radiogenic isotope data

Lead isotope data suggest a similar source for felsic dikes and ore-related sulfide minerals and overlap the ca. 70 Ma igneous rock types within the Kuskokwim basin and cinnabar and stibnite in the widespread epizonal vein systems (Szumagala, 1996; Gray et al., 1997). Shale from the Kuskokwim Group falls in the same isotopic field, but coarser (and more clastic) sedimentary rocks are more radiogenic. Therefore, lead, and by inference the coevally precipitated gold, in the Donlin Creek deposit ultimately may have been sourced in melts intruded into the basin or in the finer grained sedimentary strata. The radiogenic character of lead in the Donlin Creek gold veins is, however, only consistent with a very limited contribution from the contemporaneous mantle or lower crust into the hydrothermal system; the fine-grained Kuskokwim Group rocks thus appear to be the most likely metal source reservoir.

The Nd-Sm and Sr data (Fig. 12) indicate that, in agreement with Miller and Bundzten (1994), the felsic dikes at the Donlin Creek deposit are crustal and evolved melts originating

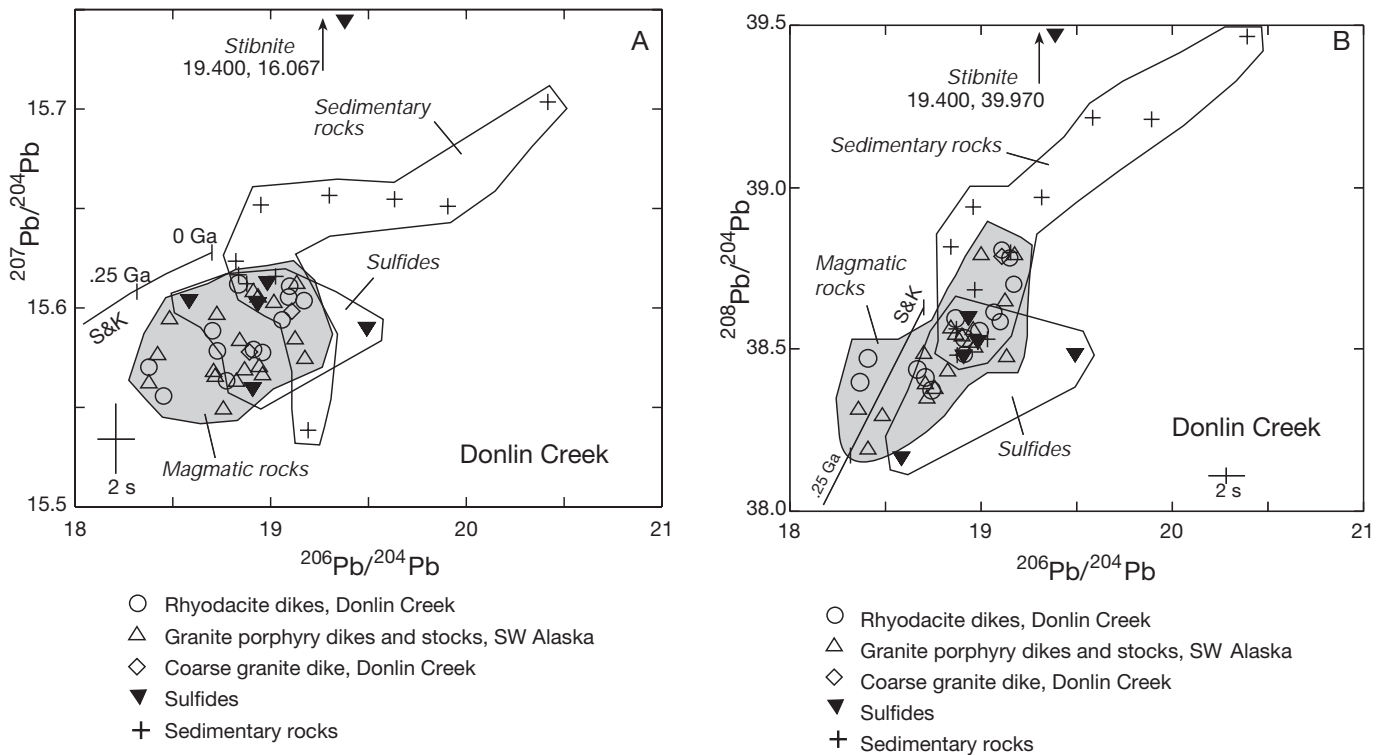


FIG. 14. Diagrams showing initial lead isotope variations of volcanic and sedimentary rocks, and sulfide minerals from Donlin Creek and from elsewhere in southwestern Alaska. A. $^{206}Pb/^{204}Pb$ vs. $^{207}Pb/^{204}Pb$. B. $^{206}Pb/^{204}Pb$ vs. $^{208}Pb/^{204}Pb$. Average crustal lead evolution curve (S&K) is from Stacey and Kramers (1975).

TABLE 7. Th-U-Pb Isotope Data for Rocks and Sulfides from the Donlin Creek Gold Deposit and from Elsewhere in Southwestern Alaska

Sample no.	Th (ppm)	U (ppm)	Pb (ppm)	²⁰⁶ Pb/ ²⁰⁴ Pb	²⁰⁷ Pb/ ²⁰⁴ Pb	²⁰⁸ Pb/ ²⁰⁴ Pb	Sample descriptions
Rhyodacite/granite porphyry dike, Donlin Creek							
DC95-175-129.8	5.78	3.64	36.00	na	na	na	Fresh rhyodacite; Vortex prospect
DC97-398-157.3	4.89	4.95	49.91	na	na	na	Rhyodacite, aphanitic; porphyritic; ACMA prospect
DC97-437-266	9.78	10.74	12.19	na	na	na	Rhyodacite; Nuno prospect
DC98-478-32-2	7.85	4.42	10.51	na	na	na	Rhyodacite, aphanitic; porphyritic; Lewis prospect
DC98-478-90	9.17	3.68	20.94	na	na	na	Rhyodacite, aphanitic; porphyritic; Lewis prospect
DC98-489-210	na	na	na	na	na	na	Altered rhyodacite; South Lewis prospect
DC98-489-210, r	na	na	na	19.166	15.604	38.705	Altered rhyodacite; South Lewis prospect
DC98-489-210, l	na	na	na	18.907	15.580	38.486	Altered rhyodacite; South Lewis prospect
DC98-387-382.5	7.47	3.11	20.02	na	na	na	Granite porphyry dike, Duqum prospect
DC98-387-382.5, r	na	na	na	19.006	15.584	38.544	Granite porphyry dike, Duqum prospect
DC98-387-382.5, l	na	na	na	19.222	15.603	38.798	Granite porphyry dike, Duqum prospect
Other granite porphyry dikes and stocks, SW Alaska							
98AM-270	8.05	5.65	14.18	na	na	na	Granite porphyry on ridge, head of Julian Ck.
98AM-271	6.29	3.59	23.06	na	na	na	Rhyolitic porphyritic dike, Julian Ck. area
98AM-271 r	na	na	na	19.059	15.576	38.537	Rhyolitic porphyritic dike, Julian Ck. area
98AM-271 l	na	na	na	18.821	15.574	38.411	Rhyolitic porphyritic dike, Julian Ck. area
98AM272	4.96	3.35	23.73	na	na	na	Granite porphyry on ridge, head of Julian Ck.
98AM-273	6.03	3.04	54.61	na	na	na	Altered feldspar-quartz porphyry, Granite Ck.
98AM-273, r	na	na	na	19.165	15.587	38.667	Altered feldspar-quartz porphyry, Granite Ck.
98AM-273, l	na	na	na	18.760	15.569	38.364	Altered feldspar-quartz porphyry, Granite Ck.
98AM-274	8.40	1.99	24.98	na	na	na	Granite porphyry, Barometer Mtn.
98AM-274 r	na	na	na	18.881	15.567	38.445	Granite porphyry, Barometer Mtn.
98AM-274 l	na	na	na	19.188	15.616	38.488	Granite porphyry, Barometer Mtn.
98AM-275A	9.58	3.81	18.72	na	na	na	Fresh, Stuyahok trenches
98AM-275A, r	na	na	na	18.874	15.605	38.606	Fresh, Stuyahok trenches
98AM-275B	9.88	3.03	202.52	na	na	na	Highly altered, Stuyahok trenches
98AM-275B, r	na	na	na	18.876	15.570	38.560	Highly altered, Stuyahok trenches
98AM-275B, l	na	na	na	18.850	15.585	38.581	Highly altered, Stuyahok trenches
98AM-276A	12.91	5.13	28.74	na	na	na	Altered, ridge above Gold Run
98AM-276A, r	na	na	na	19.306	15.581	38.817	Altered, ridge above Gold Run
98AM-277	12.17	4.53	38.68	na	na	na	Fresh, coarse granite ridge above Gold Run
98AM-277, r	na	na	na	19.046	15.571	38.582	Fresh, coarse granite ridge above Gold Run
98AM-277, l	na	na	na	18.848	15.554	38.400	Fresh, coarse granite ridge above Gold Run
Sedimentary rocks							
98AM-269	4.70	1.92	na	na	na	na	Graywacke, Kuskokwim Gr., east of Donlin Ck.
98AM-269, r	na	na	na	19.582	15.637	38.966	Graywacke, Kuskokwim Gr., east of Donlin Ck.
98AM-269, l	na	na	na	18.966	15.586	38.530	Graywacke, Kuskokwim Gr., east of Donlin Ck.
98AM-269, r	na	na	na	20.434	15.694	39.447	Graywacke, Kuskokwim Gr., east of Donlin Ck.
98AM-269, l	na	na	na	19.012	15.636	38.694	Graywacke, Kuskokwim Gr., east of Donlin Ck.
98AM270B, r	na	na	na	19.352	15.657	38.972	Silty shale, southeast of Julian Ck.
98AM270B, l	na	na	na	18.926	15.623	38.595	Silty shale, southeast of Julian Ck.
98AM-278A	8.11	3.80	22.32	na	na	na	Shale, cliff along Kuskokwim River
98AM278A, r	na	na	na	19.314	15.539	38.794	Shale, cliff along Kuskokwim River
98AM278A, l	na	na	na	18.997	15.611	38.565	Shale, cliff along Kuskokwim River
98AM278B, r	na	na	na	20.023	15.653	39.263	Sandstone, cliff along Kuskokwim River
98AM278B, l	na	na	na	19.161	15.612	38.614	Sandstone, cliff along Kuskokwim River
Sulfide minerals, Donlin Creek deposit							
97-448-65.5, pyrite, l	na	na	na	19.495	15.589	38.480	Pyrite, (in rhyodacite)
97-448-65.5, pyrite, r	na	na	na	18.913	15.559	38.476	Pyrite, (in rhyodacite)
98-456-270, stibnite, l	na	na	na	18.934	15.602	38.595	Stibnite, (in mafic dike)
98-456-270, stibnite, r	na	na	na	19.400	16.067	39.970	Stibnite, (in mafic dike)
DC98489-297.26, stibnite, l	na	na	na	18.582	15.603	38.164	Stibnite, (in mafic dike)
DC98489-297.26, stibnite, r	na	na	na	18.980	15.612	38.524	Stibnite, (in mafic dike)

Abbreviations: l = leach, na = not analyzed, r = residue

TABLE 8. Rb-Sr Isotope Data for Igneous and Sedimentary Rocks from the Donlin Creek Gold Deposit and from Elsewhere in Southwestern Alaska (for sample descriptions see Table 6)

Sample no.	Rb (ppm)	Sr (ppm)	Rb/Sr	$^{87}\text{Sr}/^{86}\text{Sr}$ (measured)	Error (2σ)
Rhyodacite/granite porphyry dike, Donlin Creek					
DC95-175-129.8	127.8	144.3	0.89	0.709275	0.000010
DC97-398-157.3	108.0	40.2	2.69	0.716045	0.000012
DC97-437-266	129.5	102.0	1.27	0.710893	0.000009
DC98-478-32-2	150.2	50.4	2.98	0.715861	0.000010
DC98-478-90	116.5	213.4	0.55	0.707125	0.000007
DC98-489-210	116.0	214.0	0.54	0.707689	0.000009
DC98-387-382.5	84.0	460.1	0.18	0.706784	0.000009
Other granite porphyry dikes and stocks, SW Alaska					
98AM-270	123.5	96.7	1.28	0.711465	0.000006
98AM272	120.9	245.4	0.49	0.708528	0.000007
98AM-273	84.8	204.6	0.41	0.708220	0.000008
98AM-274	84.9	255.3	0.33	0.706361	0.000008
98AM-275A	4.4	70.4	0.06	0.705381	0.000008
98AM-275B	82.0	15.3	5.36	0.719791	0.000009
98AM-276A	120.6	78.9	1.53	0.709208	0.000007
98AM-277	105.9	198.5	0.53	0.705851	0.000006
Sedimentary rocks					
98AM-269	47.6	94.2	0.51	0.714034	0.000009
98AM-278A	109.6	48.8	2.25	0.725903	0.000006

from mature, thickened crust. This may not be the case regionally, however, for the entire group of gold-mineralized, felsic porphyry dikes. As noted above, gold-enriched felsic dikes at occurrences such as Stuyahok (this study) and Vinasale (Szumigala, 1993) have ϵ_{Nd} of ~ 0 and $^{87}\text{Sr}/^{86}\text{Sr}$ of ~ 0.704 to 0.705 , consistent with an immature arc source characterized by a higher proportion of rocks genetically linked to the mantle. This notion is further supported by ϵ_{Nd} data for felsic dikes and rocks of the volcanic-plutonic complexes for the entire Kuskokwim region (Szumigala, 1993), with ϵ_{Nd} from -4 and $+1$. A large mantle contribution into a given melt does not correlate with gold volume in an igneous rock body; rather, structural traps for postcrystallization mineralizing fluids may have been the most important feature that localized the gold mineralization within any specific dike complex in the Kuskokwim basin.

The Nd-Pb isotope values of igneous rocks at Donlin Creek, and for roughly age-equivalent Late Cretaceous igneous rocks from terranes flanking the Kuskokwim basin, suggest fundamental differences in the deep crust of interior Alaska. The ϵ_{Nd} values range from about 0 to -10 at Donlin Creek and elsewhere in the Kuskokwim basin, higher than for granitic plutons from the Ruby and Angayucham terranes (Fig. 13A), which are immediately to the north and have ϵ_{Nd} mostly lower than -10 (Arth et al., 1989a). Values for Cretaceous and Tertiary granitic plutons to the northeast in the gold-rich (e.g., Fairbanks district) Yukon-Tanana terrane (also with ϵ_{Nd} lower than -10), as well as tonalitic and granitic gneisses and amphibolites from the Precambrian Kilbuck terrane to the south (Moll-Stalcup, 1994), can be attributed to ancient crustal reservoirs. We thus can eliminate this type of ancient and fractionated crustal reservoir as the source of the melts at Donlin Creek. In addition, lead isotope crustal

reservoirs associated with granites in the Ruby, Angayucham, and Yukon-Tanana terranes and farther northwest on the Seward Peninsula are too radiogenic and therefore also incompatible with igneous rocks at Donlin Creek (Fig. 15). Volcanic rocks from the Yukon-Koyukuk basin (including the Chisana volcanic rocks), also north of the Kuskokwim basin, are linked to the mantle by virtue of their positive ϵ_{Nd} values (Moll-Stalcup and Arth, 1991; Aleinikoff et al., 2000). Their much higher ϵ_{Nd} , when compared to the Donlin Creek dikes, define what should be the mantlelike signature for Cretaceous-Tertiary melts in interior Alaska.

Negative ϵ_{Nd} values for the Donlin Creek dikes eliminate a direct association with juvenile, mantle-derived rocks and help to characterize the type of crustal contribution to magmatism that was coeval with the gold-forming event. The T_{dm} values at Donlin Creek are substantially older than Cretaceous (i.e., >500 Ma) and allow for contributions of crust as old as 2 Ga (Fig. 13B), but one that was less fractionated for Sm/Nd than the Ruby, Angayucham, and Yukon-Tanana terranes (Fig. 13A). Lead data also eliminate a major contribution from ancient, granulite-type lower crust (no enrichment of $^{208}\text{Pb}/^{204}\text{Pb}$ relative to $^{206}\text{Pb}/^{204}\text{Pb}$), but the $^{207}\text{Pb}/^{204}\text{Pb}$ results allow a minor contribution from the mantle (as underplated mafic rocks at the base of the crust) in the Donlin Creek area (Fig. 15). Jurassic to Cretaceous Kahiltna terrane flysch and Gravina-Nutzotin belt flysch (Aleinikoff et al., 2000) overlap the neodymium and lead isotope compositions of the Donlin Creek dikes but are significantly more homogeneous for neodymium. The deep crust in the Donlin

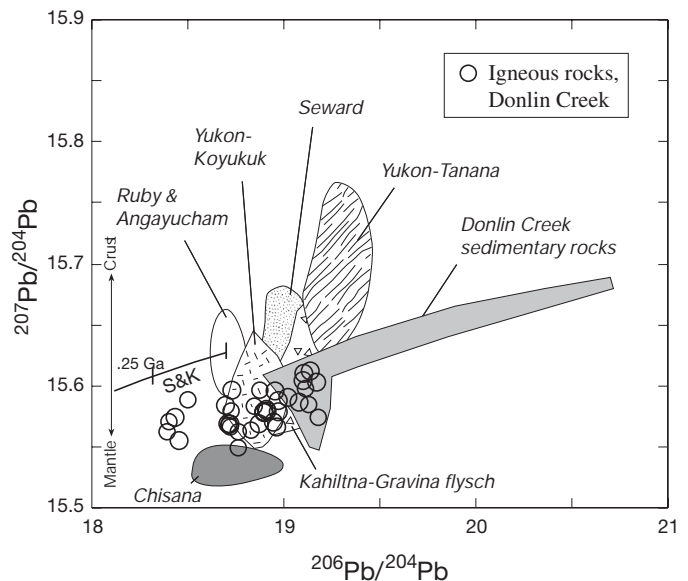


FIG. 15. Plot of initial lead isotope variations of volcanic and plutonic rocks from the Donlin Creek and other felsic dikes in the Kuskokwim basin, using $^{206}\text{Pb}/^{204}\text{Pb}$ vs. $^{207}\text{Pb}/^{204}\text{Pb}$. Isotopic fields for igneous and metamorphic rocks from adjacent terranes are shown for comparison: Cretaceous granitic plutons from the Ruby, Angayucham, and Yukon-Koyukuk terranes (Arth et al., 1989a-b), Cretaceous granitic rocks from the Seward terrane (R. Ayuso, unpub. data), Cretaceous and Tertiary granitic plutons from the Yukon-Tanana terrane (Aleinikoff et al., 2000), Jurassic to Cretaceous flysch from the Kahiltna and Gravina-Nutzotin belts (Aleinikoff et al., 2000), and Cretaceous Chisana volcanic rocks (Aleinikoff et al., 2000). Average crustal lead evolution curve (S&K) is from Stacey and Kramers (1975).

Creek area, therefore, more closely resembles the crust under the Koyukuk terrane, as characterized by neodymium and lead isotope compositions of Cretaceous plutons (Arth et al., 1989b). Both areas exhibit nearly identical ranges of ϵ_{Nd} and greatly overlap in their lead isotope values (especially in $^{207}Pb/^{204}Pb$), although the T_{dm} values for Donlin Creek point to additional contributions from older rocks than in the Koyukuk terrane (<1.5 Ga).

In summary, radiogenic isotope data indicate that (1) lead in the Donlin Creek gold ores, in regional epizonal mercury lodes, and in granitoids throughout the Kuskokwim basin has a similar source; (2) the felsic dikes at Donlin Creek predominantly represent melted, fine-grained sedimentary rocks of the Kuskokwim basin; and (3) in contrast to Donlin Creek, many of the other granite porphyry dikes and stocks in the basin have a significant mantle component. This is consistent with the model of Bundtzen and Miller (1997) that invokes intrusion of mantle melts to form the volcanic-plutonic complexes and to melt lower parts of the Kuskokwim basin. Many felsic dikes, including those at Donlin Creek, were at least partial products of this crustal melting.

Discussion

Previous classifications of the Donlin Creek gold deposit

Detailed genetic models or a specific classification of the Donlin Creek gold deposit remain problematic. Goldfarb et al. (1990), using data collected from samples of the exposed historic Snow Gulch prospect at Donlin Creek and many of the regional Hg-Sb deposits, suggested that sulfur and ore fluids were derived from sedimentary rocks within the deeper parts of the >10-km-thick Kuskokwim basin. They indicated that $\delta^{18}O$ values for meteoric water at ca. 70 Ma would be about -20 per mil and thus water/rock ratios of 0.01 or less would be required to obtain estimated fluid $\delta^{18}O$ values that were some 25 to 30 per mil higher. It is unlikely, however, that such a rock-dominated flow system could have transported the many millions of ounces of gold into the Donlin Creek deposit without much of the immense fluid volume being involved in hydration reactions along the required diffuse flow pathway (e.g., Yardley, 1997). Rather, the concentration of >20 Moz Au within the competent dike rocks at the southern part of the Donlin Creek deposit suggests a high water/rock regime, such that flow was highly focused. It is possible that the same poorly understood pathway for the crustal melts at the deposit also served as the fluid conduit.

Because of the consistently high $\delta^{18}O$ values for all the Kuskokwim region lode deposits, Goldfarb et al. (1990) interpreted the low δD from the Red Devil mercury deposit as a product of devolatilization, particularly of organic matter and fine-grained sedimentary rocks, driven by a metamorphic or magmatic heat source (e.g., organic water of Sheppard, 1986). Low-salinity fluid inclusions were quoted as evidence against the involvement of basinal connate waters for metal deposition in the studied epithermal Hg-Sb lode systems.

Bundtzen and Miller (1997) suggested that Donlin Creek and other Hg-, Sb-, and Au-bearing lodes of southwestern Alaska were genetically related to the Late Cretaceous-early Tertiary magmatism. They argued that these lodes possessed features similar to those of the alkalic-rock-related gold

deposits of the Rocky Mountain region (e.g., Kelley and Ludington, 2002). Gray et al. (1997), in an additional regional study, considered ore-forming fluids for the Donlin Creek and other deposits to have been derived from a complex mixing of metamorphic, connate, evolved meteoric water, and magmatic sources. They presented oxygen isotope data that left little doubt of the involvement of meteoric water at both the Red Top epithermal mercury deposit (300 km south of Donlin Creek) and at the nearby Granite Creek gold prospect (Fig. 1), which is geologically similar to the Donlin Creek deposit. Ebert et al. (2000a) noted that much of the Donlin Creek deposit resembled a low-sulfidation epithermal system, although the Dome prospect showed features more characteristic of an intrusion-related gold deposit (e.g., Lang and Baker, 2001). Together, these observations have been used to further suggest the possibility that boiling of deeper fluids, now preserved in fluid inclusions at the Dome prospect, led to escape of a low-density vapor phase that transported the bulk of the gold now in the southern part of the Donlin Creek deposit (Ebert et al., 2003b). Hart et al. (2002) termed Donlin Creek a high-level, epizonal gold deposit with an uncertain genetic link to magmatism.

Comparison of the Donlin Creek deposit to existing gold deposit models

Significant differences exist between the Donlin Creek deposit and typical epithermal gold deposits (e.g., Cooke and Simmons, 2000; Hedenquist et al., 2000). Gold-depositing fluids are consistently CO_2 poor in epithermal systems, although it has been long recognized that below epithermal ore zones, CO_2 can be present in significant amounts that are then lost by boiling (Henley, 1985). Nevertheless, microthermometric observations of gas hydrate and solid CO_2 crystallization during freezing experiments, indicative of perhaps 3 to 7 mol percent gas in the Donlin Creek ore fluids, are rarely reported in the literature on epithermal deposits. Although there are exceptions, in the deeper parts of many low-sulfidation epithermal systems, commonly at maximum depths of 300 to 800 m, base metal sulfide minerals are typical and Ag/Au exceeds 1.0. At the Donlin Creek deposit, which is estimated to have formed at 1 to 2 km, Au/Ag ≥ 1 and there is a lack of base metal enrichment, although copper-rich stockworks at the Dome prospect may or may not be related to the gold ores (see below). The Donlin Creek ore fluids are also distinctly enriched in ^{18}O compared to epithermal gold deposits (Fig. 11), although it might be argued that because Donlin Creek formed at slightly deeper levels than most epithermal deposits, it was less likely to have undergone significant mixing with isotopically light meteoric water.

There are also clear differences between the Donlin Creek deposit and Carlin-type gold deposits as defined by Hofstra and Cline (2000). The latter typically formed at lower temperatures (120°–180°C) and from fluids of lower gas content (1–4 mol % CO_2). The common late, low-temperature opaline silica and chalcedony in Carlin deposits are not common at Donlin Creek. The depths of ore formation are similar, widespread kaolinite is present in both systems, and shallow vein textures appear locally at Donlin Creek, but the broader range in $\delta^{18}O$ for the Carlin-like ores (Fig. 11) suggests a greater involvement of meteoric water. Gold/silver ratios

between 3 to 20, anomalous Ba, Te, and W in some ore zones, and gold-bearing pyrite that characterizes the Carlin deposits all are distinct from features observed in the Donlin Creek gold ores. Although sulfidation and silicification are recognized in both systems, argillic alteration of silicates is restricted to the Carlin deposits.

Geological and geochemical characteristics of the Donlin Creek deposit most closely resemble those associated with both orogenic and intrusion-related gold deposit types. Features consistent with the orogenic gold deposit model of Groves et al. (1998) include an association with placer accumulations, an Ag-As-Au-Hg-Sb geochemical signature that reflects sulfide complexing of metals, low base metal content of the gold resource, significant CO₂ within the ore-forming fluid, Au/Ag of unity or slightly higher, isotopically heavy oxygen in the ore fluids, a sericite-carbonate-pyrite alteration assemblage, and localization of ores in a zone of high structural competency contrast. As with most Phanerozoic orogenic gold deposits (e.g., Goldfarb et al., 2001), the Donlin Creek deposit formed in sedimentary rocks within an active collisional margin late during a period of regional strike-slip tectonism. The association of organic material with orogenic gold deposits is also common where ore fluids may be produced by metamorphic devolatilization of sedimentary rocks (e.g., Bierlein and Crowe, 2000). The broad range in estimated fluid δD at Donlin Creek (-120 to -50 per mil) is problematic. It could represent variable contributions from meteoric water, but the lack of notably low $\delta^{18}O_{\text{quartz}}$ suggests that much of the variation could record variable fluid input to the hydrothermal system from devolatilization of organic matter (cf. Sheppard, 1986). The low trapping pressures and brittle nature of the ore zones indicate that, if Donlin Creek is classified as an orogenic gold deposit, it would be of the epizonal subtype (e.g., Gebre-Mariam et al., 1995; Groves et al., 1998; Hart et al., 2002).

Alternatively, ore deposition at temperatures of 275° to 300°C and depths of 1 to 2 km supports extremely high geothermal gradients in this part of the Kuskokwim basin. This might warrant the classification of the Donlin Creek deposit as an intrusion-related gold deposit (e.g., Thompson et al., 1999; Lang and Baker 2001), a deposit type whose features are difficult to distinguish from those of more widely recognized orogenic gold deposits (Sillitoe and Thompson, 1998). If Donlin Creek is indeed an intrusion-related gold deposit, then the causative intrusion remains to be recognized. One possibility is that the intrusion is buried beneath the hornfels Kuskokwim Group rocks at the Dome prospect. However, given the anatectic nature of many of the granitoids in southwestern Alaska, it might be impossible to tell whether the ore fluids evolved during prograde metamorphism of the flysch in the deforming basin (possibly caused by rising mantle magma) or if they were exsolved from a magma that formed from the melting of the flysch. In such circumstances, where high temperatures produce both devolatilization and then melting of a sequence of sedimentary rocks, a distinction between intrusion-related and orogenic gold deposit types is difficult.

Preferred genetic model

The Kuskokwim flysch basin that hosts the Donlin Creek deposit formed during a ca. 20-m.y.-long interval in the Late

Cretaceous. The continental crust that formed the basement of the basin had only recently been assembled from continental fragments (Farewell and Kilbuck terranes), an island arc (Togiak terrane), and obducted ocean floor (Innoko terrane). The basin formed in the continental back-arc above a roughly north- or northwest-dipping subduction zone along Alaska's Pacific margin. Donlin Creek was probably located about 500 km landward of the paleotrench.

The 70 Ma age of the Donlin Creek deposit is noteworthy for several reasons. First, an exceptionally wide and vigorous arc evolved at this time (Alaska Range and Kuskokwim Mountains belts of Wallace and Engebretson, 1984). Second, gold and mercury mineralization developed across a wide zone in southwestern Alaska (Bundtzen and Miller, 1997). Third, both the Iditarod and Denali fault systems appear to have undergone dextral displacement at ca. 70 Ma (Miller et al., 2002). Finally, at Donlin Creek and other locations between the regional strike-slip faults, lower order structures record roughly north-south compression at ca. 70 Ma, which would seem to be more compatible with sinistral strike-slip on the two master faults (Ebert et al., 2000a). If such a pulse of sinistral motion did take place on the Iditarod fault (as favored by Ebert et al., 2002a), it would have been no more than a momentary reversal of motion on a long-lived dextral system. Alternatively, the complex system of structures at Donlin Creek may reflect the interplay between northward coast-parallel terrane transport along the Canadian margin to the southeast (itself the product of dextral-oblique convergence) and roughly orthogonal subduction beneath southwestern Alaska (Miller et al., 2002). The possibility exists that by 70 Ma, southwestern Alaska was being affected by the approach of the Kula-Resurrection (or Kula-Farallon) spreading ridge and its attendant slab window (Bradley et al., 2003). More likely, however, this did not happen until ca. 63 Ma.

Mantle melts formed throughout the Maastrichtian in the wedge above the subducting slab (e.g., Moll-Stalcup, 1994) and below the 30- to 35-km-thick crust (Barnes, 1977). The upper part of this crust, defined by the Kuskokwim flysch, may have exceeded 10 km in thickness by the end of basin sedimentation at ca. 70 Ma. The mantle melts, which were significantly contaminated by the overlying crustal rocks through which they passed (Moll-Stalcup, 1994), reached the surface and near-surface in many parts of the Kuskokwim basin and also are spatially associated with hornfels in the flysch. More local flysch melts are evidenced by some dike swarms, such as the ca. 70 Ma swarm that hosts the ore at Donlin Creek.

Isotope and fluid inclusion data are consistent with a number of feasible ca. 70 Ma ore fluid sources within the Kuskokwim basin (Fig. 16). The relatively competent rocks of the crustally derived felsic dike swarm provided a favorable structural host for the gold ores, and fluid exsolution from deeper parts of the same crustal melt reservoir is one possible mechanism for ore formation. An alternative scenario is that the fluids were released from broad-scale devolatilization reactions triggered by the rising geotherms above the mantle melts; these mantle magmas would thus have been responsible for both flysch melts and fluid generation in the deeper parts to the Kuskokwim basin. The extremely depleted $\delta^{34}S$ values of the ore-related sulfide minerals, however, are

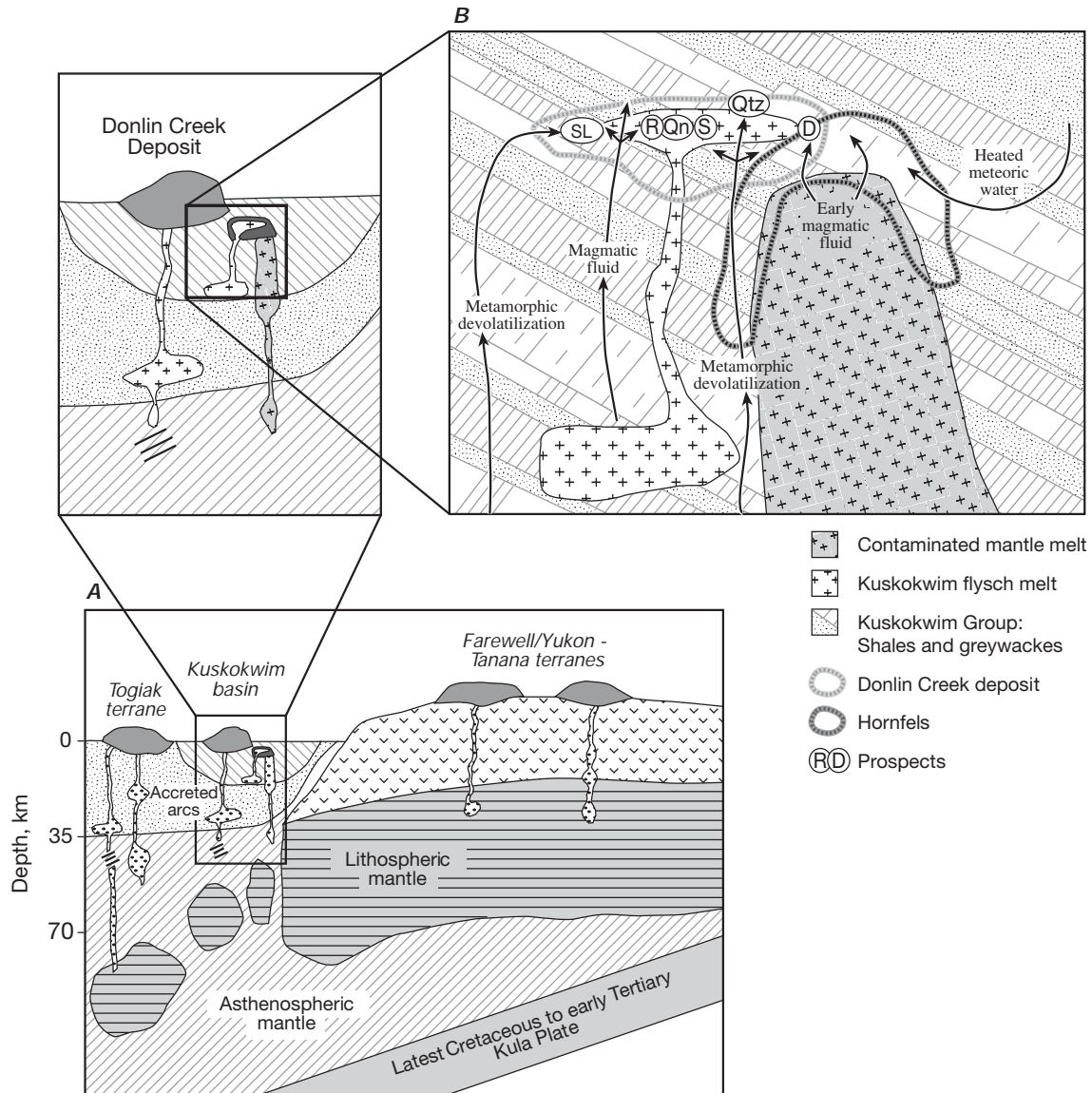


FIG. 16. Genetic model for evolution of the Donlin Creek gold deposit with crustal structure generalized after Moll-Stalcup and Arth (1989) and Gray et al. (1997). A. Partial mantle melting above the subducting Kula plate led to the emplacement of crustally contaminated intrusions and volcanic-plutonic complexes throughout the Kuskokwim basin. In a few locations, and including at the site of the Donlin Creek deposit, small, almost pure flysch melts evolved. B. Gold-transporting hydrothermal fluids were released during devolatilization of flysch deep in the Kuskokwim basin and/or from the flysch melts themselves. It is uncertain as to whether minor amounts of surface waters also entered the hydrothermal system. The fluids localized the gold-bearing veins in the already crystallized and structurally competent, flysch-melt dike-sill complex at Donlin Creek (e.g., forming prospects that include South Lewis (SL), Rochilieu (R), Queen (Qn), Snow (S), Quartz (Qtz), Dome (D)). A high-temperature, early magmatic copper-gold vein set at the Dome prospect, which was subsequently overprinted by the main-stage Donlin Creek gold event, is spatially associated with a hornfels zone perhaps indicative of a relatively extensive buried plutonic body.

incompatible with magmatic fluids that are derived from melts with a strong mantle component, which are common elsewhere throughout the Kuskokwim basin. If the ore fluids were from a magmatic fluid source, then such a source melt must have been mainly anatectic in nature. Hydrogen and oxygen isotope data indicate that some meteoric water component may have mixed with the deeper crustal hydrothermal system, but it was of minor significance.

The circulating hydrothermal fluids were focused into brittle fractures, which were localized in low-order dilational zones adjacent to local strike-slip faults (i.e., Donlin Creek fault) in the Kuskokwim basin. The relatively competent, coeval to slightly older (by no more than a few million years) felsic dikes at Donlin Creek were the site of the associated north-south-directed compression during the ongoing far-field dextral strike-slip on the more regional faults.

High-temperature (400°–550°C) chalcopyrite-bearing auriferous veins at the Dome prospect were deposited from a high-salinity fluid near a magmatic source, as supported by their localization within the hornfels area. Despite equivocal age data, crosscutting relationships with pyrite-arsenopyrite-stibnite-gold veins (Ebert et al., 2000a) indicate that the chalcopyrite-bearing veins predated the main gold event. The auriferous arsenopyrite-bearing veins at the ca. 70 Ma prospects in the southern part of the Donlin Creek deposit were subsequently deposited from low-salinity fluids, at about 275° to 300°C and 1 to 2 km. Pressure fluctuations leading to episodic H₂S release from a typically homogeneous fluid may have been critical for gold precipitation; less commonly, episodic unmixing of CO₂ also from the H₂O-dominant ore fluids may have further enhanced gold destabilization and precipitation. Other arsenic-bearing mineral phases and stibnite, with at least the sulfur in the associated fluids coming from a slightly different reservoir within the Cretaceous flysch sequence, overprinted the gold-arsenopyrite assemblage at lower temperatures.

Significance of the Dome prospect

The genetic relationship between the Dome prospect and the main Donlin Creek gold resource is still uncertain. The $\delta^{34}\text{S}$ data for sulfide minerals from Dome, like those from all of the Donlin Creek deposit, are very low and suggest sulfur derivation from the flysch basin. Relatively higher fluid inclusion homogenization temperatures, as well as lower $\delta^{18}\text{O}$ values for quartz at Dome, are consistent with a higher temperature hydrothermal system during copper and oldest gold deposition. But whether the Dome hydrothermal system cooled and evolved into the main gold depositing system at the Donlin Creek deposit is unclear. The difference in fluid inclusion eutectic temperatures between the Dome and the Donlin Creek gold veins, suggestive of significant magnesium in the former, argues against a single fluid reservoir.

Analogous deposits in the northern Cordillera and elsewhere

As noted by Hart et al. (2002), the Donlin Creek deposit is one of three epizonal systems in the Tintina gold province of interior Alaska and Yukon. These three high-level hydrothermal systems also included the presently producing True North deposit in the Fairbanks district in eastern Alaska and the previously mined Brewery Creek deposit near Dawson City, Yukon. As with the Donlin Creek deposit, these other two gold deposits formed at shallow (1–2 km) levels, causing some workers to define them as high-level intrusion-related gold deposits (e.g., Lang and Baker, 2001), but causative plutons have yet to be identified. Similarities between True North, Brewery Creek, and Donlin Creek include the As-Au-Hg-Sb geochemical signature, the carbonaceous nature of the ores, the refractory nature of the gold within arsenopyrite and/or arsenian pyrite rims, and the brittle style of quartz sulfide mineral fracture networks. In contrast to the Kuskokwim region, the Fairbanks and Dawson City areas were not glaciated and thus gold released during oxidation of the auriferous sulfide minerals in the True North and Brewery Creek deposits had been concentrated as economic targets at shallow depths. Thus, development of the Donlin Creek deposit

in the near future would represent the first successful mining of a high-tonnage, solely hypogene epizonal deposit in the northern Cordillera.

The Dome prospect has a number of similarities to the Shotgun deposit located 400 km to the south within the Kuskokwim basin. As described by Rombach and Newberry (2001), auriferous quartz stockworks and breccia at Shotgun, resembling a porphyry-style system, cut a ca. 70 Ma granite porphyry stock and mineralizing fluids are, for the most part, similar in chemistry to those reported here for the Dome prospect. In contrast to Dome, the Shotgun deposit is characterized by a high Ag/Au ratio (4/1), arsenopyrite >> chalcopyrite, significant molybdenum (avg 40 ppm Mo), tungsten-bearing ore phases, important albite alteration, a high sodium (rather than Mg-K) concentration in the hydrothermal fluids, and igneous (rather than in hornfels) host rocks. Both hydrothermal systems may, however, be relatively high temperature magmatic occurrences and are possibly associated with the same ca. 70 Ma intrusive episode.

On a global scale, deposits that are comparable to Donlin Creek are likely in marine sedimentary rock-dominant terranes along active continental margins. Many sedimentary rock-hosted, large-tonnage, auriferous quartz veinlet systems in northeastern Russian (e.g., Maiskoe, Sarylakh, Kyuchus; Volkov et al., 2002), which are enriched in arsenic, antimony, and commonly mercury, may be analogs of Donlin Creek.

The still active hydrothermal systems and associated silica-carbonate mercury deposits in the Sonoma-Clear Creek volcanic fields of western California (e.g., Rytuba, 1993, and papers therein) may be modern analogs to the near-surface part of the Kuskokwim basin about 70 m.y. ago. We suggest that Donlin Creek-type gold deposits could be forming today at depths of 1 to 2 km below the surface in California. In fact, Pickthorn (1993) has even used the recognition of compositionally distinct spring chemistries to suggest that exposed hot spring-type gold deposits in these volcanic fields (e.g., McLaughlin) may be the products of remobilization of metals from slightly older gold concentrations at depth that could resemble the Donlin Creek deposit.

Exploration criteria

The enormous resource at the Donlin Creek gold deposit has only been recognized during the last decade. The obvious question is whether this world-class gold system is an anomaly or whether there are more such deposits of the same type remaining to be discovered in the Kuskokwim basin. Areas of competency contrast, provided by ca. 70 Ma igneous rocks near important structures in the flysch, as well as hornfels zones, such as at the Dome prospect, may be prospective for these types of gold systems. These features, however, are widespread in this part of Alaska and are not uniquely associated with the lode gold systems. Obvious geochemical pathfinders in stream sediment surveys would include gold, arsenic, antimony, and mercury, but many small prospects throughout southwestern Alaska yield the same signatures. Induced polarization and resistivity geophysical studies have been attempted at the Donlin Creek deposit but only seem useful once mineralized corridors are identified; they are unlikely to be helpful in identification of new targets.

A few significant anomalies identified from our studies may provide some useful features to aid in regional exploration throughout the basin and are listed below.

1. Examination of structurally, and perhaps genetically, favorable igneous rocks might be focused in boundary areas between the north-northeast- and east-west-trending structural domains. These may be the most important dilational zones within the basin that are capable of focusing large fluid volumes.

2. Radiogenic isotope data have shown that the felsic dikes at Donlin Creek are isotopically distinct from many of the other granite porphyry igneous bodies in southwestern Alaska; that is, they reflect a much greater degree of crustal melting. It is possible that areas in the basin with the greatest degree of melting may also be areas of maximum hydrothermal fluid production. If correct, then other areas of igneous rocks with exceptionally high $^{87}\text{Sr}/^{86}\text{Sr}$ and low ϵ_{Nd} may be targeted as possible sites of relatively voluminous hydrothermal activity. In fact, the higher degree of melting in the Donlin Creek area, perhaps a function of a more intense thermal event, may be critical in explaining the large deposit size.

3. The very low $\delta^{34}\text{S}$ of sulfide minerals from the Donlin Creek deposit appears unique among most of the epizonal vein deposits in the Kuskokwim basin (e.g., Goldfarb et al., 1990; Gray et al., 1997). This too may reflect a local high degree of heating of the flysch and remobilization of large amounts of sedimentary sulfur in the hydrothermal fluid. An exceptionally large sulfur reservoir in the sedimentary rocks may be a critical factor in producing such a giant gold deposit (e.g., Wilde et al., 2000). Mueller et al. (2003) showed from a hydrogeochemical survey in the Donlin Creek area that extremely low $\delta^{34}\text{S}$ values can provide a useful exploration tool for identification of Donlin Creek-type mineralization. In addition, Goldfarb et al. (1990) noted a $\delta^{34}\text{S}$ value for cinnabar of -16.5 per mil at the Mountain Top mercury deposit (100 km south of Donlin Creek). This is the only $\delta^{34}\text{S}$ value from a vein deposit in the Kuskokwim basin that is as low as the Donlin Creek sulfide minerals and could be indicative of a similar type of hydrothermal system.

Conclusions

The Donlin Creek gold deposit represents a significant new lode gold resource in a region of the northern North American Cordillera that has traditionally been a placer province for the previous 100 yr. Relatively low salinity, CO_2 -rich ore fluids are consistent with those in gold deposits throughout the metamorphosed, accreted terranes of western North America and other continental margin orogens. Such fluids have been suggested as either products of devolatilization of the sedimentary rock-dominant terranes or gas-rich magmatic fluids. Both are permissive sources for the fluids in the Donlin Creek hydrothermal system, although if the latter was important at Donlin Creek, then the sulfur isotope data indicate that the causative intrusion was one dominated by a flysch-melt component. The oxygen isotope data are compatible with a fluid of metamorphic or flysch-melt magmatic origin, although some variability is consistent with a minor input of meteoric water into the hydrothermal system at some time.

Results from this study indicate that careful examination of gold-bearing, low base metal, stibnite-rich lodes in sedimentary rock packages is warranted during any gold exploration program, particularly in regions dominated by already recognized gold deposits, whether these are lodes or, as in the Kuskokwim basin, placer deposits. Antimony-rich systems, as with many low sulfide gold deposits, are indicative of a hydrothermal system in which metal transport was dominated by bisulfide complexing. Differences in solubility with temperature between As, Au, Hg, and Sb may cause a zoning pattern such that exposed mercury- or antimony-rich lodes define the tops to large gold resources at depth. In the case of Donlin Creek, some telescoping of the deposit has overlapped antimony with gold-arsenic mineralization. A high geothermal gradient applied to a sequence of marine sedimentary rocks may inherently lead to a concentration of S, As, Au, Sb, and Hg in resulting crustally derived fluids. Emplacement of subduction-related mantle melts into the bottom of the Kuskokwim flysch basin likely provided the ultimate 70 Ma thermal engine for metal mobilization in the sedimentary rocks and the eventual concentration of a significant gold resource.

Acknowledgments

Discussions with Tom Bundtzen, Stan Dodd, Carol Finn, John Gray, Craig Hart, Dan McCoy, and Dave Szumigala regarding features of the Donlin Creek deposit added significantly to this paper. We are indebted to Robert Burruss for assistance with the Raman microprobe. Poul Emsbo contributed the reconnaissance gas-liquid chromatography. Eric Anderson helped with some of the fluid inclusion measurements. John Thompson, Pepe Perello, Cam Rombach, and Rainer Newberry are thanked for reviews of the original manuscript.

April 28, 2003; January 5, 2004

REFERENCES

- Aleinikoff, J.N., Farmer, G.L., Rye, R.O., and Nokleberg, W.J., 2000, Isotopic evidence for the sources of Cretaceous and Tertiary granitic rocks, east-central Alaska: Implications for the tectonic evolution of the Yukon-Tanana terrane: *Canadian Journal of Earth Sciences*, v. 37, p. 945–956.
- Arth, J.G., Zmuda, C.C., Foley, N.K., Criss, R.E., Patton, W.W., Jr., Miller, T.P., and Box, S.E., 1989a, Isotopic and trace element variations in the Ruby batholith, Alaska, and the nature of the deep crust beneath the Ruby and Angayucham terranes: *Journal of Geophysical Research*, v. 94, p. B15,941–B15,955.
- Arth, J.G., Criss, R.E., Zmuda, C.C., Foley, N.K., Patton, W.W., Jr., Miller, T.P., and Box, S.E., 1989b, Remarkable isotopic and trace element trends in potassic through sodic Cretaceous plutons of the Yukon-Koyukuk basin, Alaska, and the nature of the lithosphere beneath the Koyukuk terrane: *Journal of Geophysical Research*, v. 94, p. B15,957–B15,968.
- Barnes, D.F., 1977, Bouguer gravity map of Alaska: U.S. Geological Survey Map GP-913.
- Bierlein, F.P., and Crowe, D.E., 2000, Phanerozoic orogenic lode gold deposits: *Reviews in Economic Geology*, v. 13, p. 103–139.
- Bradley, D., Kusky, T., Haeussler, P., Goldfarb, R., Miller, M., Dumoulin, J., Nelson, S., and Karl, S., 2003, Geologic signature of early Tertiary ridge subduction in Alaska: *Geological Society of America Special Paper 371*, p. 19–50.
- Brown, P.E., 1989, FLINCOR: A microcomputer program for the reduction and investigation of fluid-inclusion data: *American Mineralogist*, v. 74, p. 1390–1393.
- Bull, K., 1988, Genesis of the Golden Horn and related mineralization in the Flat area, Alaska: Unpublished M.Sc. thesis, Fairbanks, Alaska, University of Alaska, 300 p.

- Bundtzen, T.K., and Miller, M.L., 1997, Precious metals associated with Late Cretaceous-early Tertiary igneous rocks of southwestern Alaska: *ECONOMIC GEOLOGY MONOGRAPH* 9, p. 242–286.
- Bundtzen, T.K., Miller, M.L., Laird, G.M., and Kline, J.T., 1985, Geology of heavy mineral placer deposits of the Iditarod and Innoko precincts, western Alaska: Alaska Placer Mining Association, 7th Annual Meeting on Placer Mining, Fairbanks, Alaska, March 27–30, 1985, Proceedings, p. 35–41.
- Cady, W.M., Hoare, J.M., Wallace, R.E., Webber, G.C., and Webber, E.J., 1955, The central Kuskokwim region, Alaska: U.S. Geological Survey Professional Paper 268, 132 p.
- Cooke, D.R., and Simmons, S.F., 2000, Characteristics and genesis of epithermal gold deposits: *Reviews in Economic Geology*, v. 13, p. 221–244.
- Decker, J., Bergman, S.C., Blodgett, R.B., Box, S.E., Bundtzen, T.K., Clough, J.G., Coonrad, W.L., Gilbert, W.G., Miller, M.L., Murphy, J.M., Robinson, M.S., and Wallace, W.K., 1994, Geology of southwestern Alaska: Geological Society of America, *Geology of North America*, v. G-1, p. 235–310.
- Decker, J., Reifensstuhl, R.R., Robinson, M.S., Waythomas, C.F., and Clough, J.G., 1995, Geology of the Sleetmute A-5, A-6, B-5, and B-6 quadrangles, southwestern Alaska: Alaska Division of Geology and Geophysical Surveys Professional Report 99, 16 p.
- DePaolo, D.J., 1981, Neodymium isotopes in the Colorado Front Range and crust-mantle evolution in the Proterozoic: *Nature*, v. 291, p. 193–196.
- Dodd, S., 1996, Donlin Creek project, southwest Alaska [abs.]: Alaska Miners Association Annual Convention, Anchorage, Alaska, November 6–8, 1996, Abstracts, p. 27–28.
- Dunne, K.P.E., 1993, Summary of fluid inclusion petrography, Lewis and Carolyn showings: Mineral Deposit Research Unit, University of British Columbia, unpublished report, 10 p.
- Ebert, S., Dodd, S., Miller, L., and Petsel, S., 2000a, The Donlin Creek Au-As-Sb-Hg deposit, southwestern Alaska: Geological Society of Nevada, *Geology and Ore Deposits 2000 Symposium*, 4th, Reno-Sparks, Nevada, May 15–18, 2000, Proceedings, p. 1069–1081.
- Ebert, S., Miller, L., Petsel, S., Dodd, S., Kowalczyk, P., Tucker, T.L., and Smith, M.T., 2000b, Geology, mineralization, and exploration at the Donlin Creek project, southwestern Alaska: British Columbia and Yukon Chamber of Mines Special Volume 2, p. 99–114.
- Ebert, S.W., Baker, T., and Spencer, R.J., 2003a, Fluid inclusion studies at the Donlin Creek gold deposit, Alaska, possible evidence for reduced porphyry-Au to sub-epithermal transition: Biennial SGA Meeting, 7th, Athens, Greece, Proceedings, p. 263–266.
- Ebert, S.W., Tosdal, R.M., Goldfarb, R.J., Ayuso, R., and Gabites, J., 2003b, The 23 million ounces Donlin Creek gold deposit, SW Alaska—a possible link between reduced porphyry Au and epizonal to epithermal Au-As-Sb-Hg mineralization [abs.]: Geological Association of Canada-Mineralogical Association of Canada, Vancouver, BC, Canada, May 25–28, 2003, Program with Abstracts, v. 28, p. 477.
- Field, C.W., and Fifarek, R.H., 1985, Light stable-isotopes systematics in the epithermal environment: *Reviews in Economic Geology*, v. 2, p. 99–128.
- Gebre-Mariam, M., Hagemann, S.G., and Groves, D.I., 1995, A classification scheme for epigenetic Archean lode-gold deposits: *Mineralium Deposita*, v. 30, p. 408–410.
- Gehrig, M., Lentz, H., Franck, E.U., and Hamilton, D.L., 1980, Phase equilibria and PVT of binary and ternary mixtures of water, carbon dioxide and sodium chloride up to 3 kb and 550 degrees C: *Mineralogical Society Bulletin*, no. 49, p. 6.
- Goldfarb, R.J., 1997, Metallogenic evolution of Alaska: *ECONOMIC GEOLOGY MONOGRAPH* 9, p. 4–34.
- Goldfarb, R.J., Gray, J.E., Pickthorn, W.J., Gent, C.A., and Cieutat, B.A., 1990, Stable isotope systematics of epithermal mercury-antimony mineralization, southwestern Alaska: U.S. Geological Survey Bulletin 1950, p. E1–E9.
- Goldfarb, R.J., Groves, D.I., and Gardoll, S., 2001, Orogenic gold and geologic time—a global synthesis: *Ore Geology Reviews*, v. 18, p. 1–75.
- Goldstein, R.H., and Reynolds, T.J., 1994, Systematics of fluid inclusions in diagenetic minerals: *Society for Sedimentary Geology Short Course* 31, 199 p.
- Gray, J.E., Frost, T.P., Goldfarb, R.J., and Detra, D.E., 1990, Gold associated with cinnabar- and stibnite-bearing deposits and mineral occurrences in the Kuskokwim River region, southwestern Alaska: U.S. Geological Survey Bulletin 1950, p. D1–D6.
- Gray, J.E., Gent, C.A., Snee, L.W., and Wilson, F.H., 1997, Epithermal mercury-antimony and gold-bearing vein lodes of southwestern Alaska: *ECONOMIC GEOLOGY MONOGRAPH* 9, p. 287–305.
- Groves, D.I., Goldfarb, R.J., Gebre-Mariam, M., Hagemann, S.G., and Robert, F., 1998, Orogenic gold deposits: A proposed classification in the context of their crustal distribution and relationship to other gold deposit types: *Ore Geology Reviews*, v. 13, p. 7–27.
- Hart, C.J.R., McCoy, D.T., Goldfarb, R.J., Smith, M., Robert, P., Hulstein, R., Bakke, A.A., and Bundtzen, T.K., 2002, Geology, exploration, and discovery in the Tintina gold province, Alaska and Yukon: *Society of Economic Geologists Special Publication* 9, p. 241–274.
- Hedenquist, J.W., Arribas R. A., and Gonzalez-Urien, E., 2000, Exploration for epithermal gold deposits: *Reviews in Economic Geology*, v. 13, p. 245–277.
- Henley, R.W., 1985, The geothermal framework of epithermal deposits: *Reviews in Economic Geology*, v. 2, p. 1–24.
- Hofstra, A.H., and Cline, J.S., 2000, Characteristics and models for Carlin-type gold deposits: *Reviews in Economic Geology*, v. 13, p. 163–220.
- Kelley, K.D., and Ludington, S., 2002, Cripple Creek and other alkaline-related gold deposits in the southern Rocky Mountains, USA: Influence of regional tectonics: *Mineralium Deposita*, v. 37, p. 38–60.
- Kerrich, R., 1989, Geochemical evidence on the sources of fluids and solutes for shear zone hosted mesothermal Au deposits: *Geological Association of Canada Short Course Notes*, v. 6, p. 129–197.
- Kyser, T.K., 1987, Equilibrium fractionation factors for stable isotopes: *Mineralogical Association of Canada Short Course Handbook*, v. 13, p. 1–84.
- Lang, J.R., and Baker, T., 2001, Intrusion-related gold systems: Then present level of understanding: *Mineralium Deposita*, v. 36, p. 477–489.
- Ludwig, K. R., 1991, PBDAT—A computer program for processing Pb-U-Th isotope data, version 1.20: U.S. Geological Survey Open-file Report 88-542.
- 1992, Isoplot—A plotting and regression program for radiogenic-isotope data, version 2.57: U.S. Geological Survey Open-file Report 91-445.
- Mattinson, J. M., 1987, U-Pb ages of zircons—a basic examination of error propagation: *Chemical Geology*, v. 66, p. 151–162.
- Matsuhisa, Y., Goldsmith, J.R., and Clayton, R.N., 1979, Oxygen isotopic fractionation in the system quartz-albite-anorthite-water: *Geochimica et Cosmochimica Acta*, v. 43, p. 1131–1140.
- Mernagh, T.P., and Trudu, A.G., 1993, A laser Raman microprobe study of some geologically important sulphide minerals: *Chemical Geology*, v. 103, p. 113–127.
- Miller, L.D., Ebert, S., Kowalczyk, P., Petsel, S., McAtee, J., Goldfarb, R., Miller, M.L., and Dodd, S., 2000, Geology, mineralization, and exploration at the Donlin Creek project, southwestern Alaska [abs.]: 17th Annual Cordilleran Exploration Roundup, Vancouver—Gateway to Discoveries, 2000, Vancouver, BC, Canada, January 25–28, 2000, Abstracts, p. 45.
- Miller, M.L., and Bundtzen, T.K., 1994, Generalized geologic map of the Iditarod quadrangle, Alaska, showing potassium-argon, major oxide, trace element, fossil, paleocurrent, and archaeological sample localities: U.S. Geological Survey Miscellaneous Field Study Map MF-2219-A, 48 p.
- Miller, M.L., Belkin, H.E., Blodgett, R.B., Bundtzen, T.K., Cady, J.W., Goldfarb, R.J., Gray, J.E., McGimsey, R.G., and Simpson, S.L., 1989, Pre-field study and mineral resource assessment of the Sleetmute quadrangle, southwestern Alaska: U.S. Geological Survey Open-file Report 89-363, 115 p.
- Miller, M.L., Bradshaw, J.Y., Kimbrough, D.L., Stern, T.W., and Bundtzen, T.K., 1991, Isotopic evidence for early Proterozoic age of the Idono Complex, west-central Alaska: *Journal of Geology*, v. 99, p. 209–223.
- Miller, M.L., Bradley, D.C., Bundtzen, T.K., and McClelland, W., 2002, Late Cretaceous through Cenozoic strike-slip tectonics of southwestern Alaska: *Journal of Geology*, v. 110, p. 247–270.
- Moll-Stalcup, E.J., 1994, Latest Cretaceous and Cenozoic magmatism in mainland Alaska: Geological Society of America, *Geology of North America*, v. G-1, p. 589–620.
- Moll-Stalcup, E., and Arth, J. G., 1989, The nature of the crust in the Yukon-Koyukuk province as inferred from the chemical and isotopic composition of five Late Cretaceous to early Tertiary volcanic fields in western Alaska: *Journal of Geophysical Research*, B, Solid Earth and Planets, v. 94, p. 15,989–16,020.
- 1991, Isotopic and chemical constraints on the petrogenesis of Blackburn Hills volcanic field, western Alaska: *Geochimica et Cosmochimica Acta*, v. 55, p. 3753–3776.
- Moll-Stalcup, E.J., Wooden, J.L., Bradshaw, J.Y., and Aleinikoff, J.N., 1996, Elemental and isotopic evidence for 2.1-Ga arc magmatism in the Kilbuck terrane, southwestern Alaska: U.S. Geological Survey Bulletin 2152, p. 111–130.
- Mueller, S.H., Goldfarb, R.J., Munk, L., Miller, M.L., Foley, J.Y., and Gemery, P.A., 2003, Sulfur isotopes in surface and groundwater sulfate as an exploration tool for epizonal gold deposits in the Kuskokwim basin, SW Alaska [abs.]: Geological Society of America, Abstracts with Programs, v. 35, p. 401.

- Newberry, R.J., Allegro, G.L., Cutler, S.E., Hagen-Levelle, J.H., Adams, D.D., Nicholson, L.C., Weglarz, T.B., Bakke, A.A., Clautice, K.H., Coulter, G.A., Ford, M.J., Myers, G.L., and Szumigala, D.J., 1997, Skarn deposits of Alaska: ECONOMIC GEOLOGY MONOGRAPH 9, p. 355–395.
- Ohmoto, H., and Goldhaber, M.B., 1997, Sulfur and carbon isotopes, in Barnes, H.L., ed., *Geochemistry of hydrothermal ore deposits*, 3rd ed.: New York, John Wiley and Sons, p. 517–612.
- Ohmoto, H., and Rye, R.O., 1979, Isotopes of sulfur and carbon, in Barnes, H.L., ed., *Geochemistry of hydrothermal ore deposits*, 2nd ed.: New York, Wiley-Interscience, p. 509–567.
- O'Neil, J.R., Shaw, S.E., and Flood, R.H., 1977, Oxygen and hydrogen isotope compositions as indicators of granite genesis in the New England batholith, Australia: *Contributions to Mineralogy and Petrology*, v. 62, p. 313–328.
- Pickthorn, W.J., 1993, Relation of hot-spring gold mineralization to silica-carbonate mercury mineralization in the Coast Ranges, California: Society of Economic Geologists Guidebook Series, v. 16, p. 77–89.
- Piekenbrock, J.R., and Petsel, S.A., 2003, Geology and interpretation of the Donlin Creek gold deposits: Juneau, Alaska, NovaGold Resources Inc., unpublished report, 58 p.
- Pokrovski, G., Gout, R., Schott, J., Zotov, A., and Harrichoury, J-C., 1996, Thermodynamic properties and stoichiometry of As(III) hydroxide complexes at hydrothermal conditions: *Geochimica et Cosmochimica Acta*, v. 60, p. 737–749.
- Pokrovski, G.S., Kara, S., and Roux, J., 2002, Stability and solubility of arsenopyrite, FeAsS, in crustal fluids: *Geochimica et Cosmochimica Acta*, v. 66, p. 2361–2378.
- Roedder, E., 1984, Fluid inclusions: *Reviews in Mineralogy*, v. 12, 644 p.
- Rombach, C.S., and Newberry, R.J., 2001, Shotgun deposit—granite porphyry-hosted gold-arsenic mineralization in southwestern Alaska, USA: *Mineralium Deposita*, v. 36, p. 607–621.
- Rytuba, J.J., 1993, Active geothermal systems and gold-mercury deposits in the Sonoma-Clear Creek volcanic fields, California: Society of Economic Geologists Guidebook Series, v. 16, 361 p.
- Sainsbury, C.L., and MacKevett, E.M., Jr., 1965, Quicksilver deposits of southwestern Alaska: U.S. Geological Survey Bulletin 1187, 89 p.
- Sheppard, S.M.F., 1986, Characterization and isotopic variations in natural waters: *Reviews in Mineralogy*, v. 16, p. 165–183.
- Sillitoe, R.H., and Thompson, J.F.H., 1998, Intrusion-related vein gold deposits: Types, tectono-magmatic settings and difficulties of distinction from orogenic gold deposits: *Resource Geology*, v. 48, p. 237–250.
- Stacey, J.S., and Kramers, J.D., 1975, Approximation of terrestrial lead isotope evolution by a two-stage model: *Earth and Planetary Science Letters*, v. 26, p. 207–221.
- Swainbank, R.C., Szumigala, D.J., Henning, M.W., and Pillifant, F.M., 2001, Alaska's mineral industry 2001: Alaska Division of Geological and Geophysical Surveys Special Report 56, 65 p.
- Szumigala, D.J., 1993, Gold mineralization related to Cretaceous-Tertiary magmatism in the Kuskokwim Mountains of west-central and southwestern Alaska: Unpublished Ph.D. dissertation, Berkeley, California, University of California, 301 p.
- 1996, Gold mineralization related to Cretaceous-Tertiary magmatism in west-central Alaska: A geochemical model and prospecting guide for the Kuskokwim region: Geological Society of Nevada Ore Deposits of the American Cordillera Symposium, Reno-Sparks, Nevada, April 10-13, 1995, Proceedings, p. 1317–1340.
- Szumigala, D.J., Dodd, S.P., and Arribas, A., Jr., 2000, Geology and gold mineralization at the Donlin Creek prospects, southwestern Alaska: Alaska Division of Geological and Geophysical Survey Professional Report 119, p. 91–115.
- Taylor, H.P., Jr., and Sheppard, S.M.F., 1986, Igneous rocks: I. Processes of isotopic fractionation and isotope systematics: *Reviews in Mineralogy*, v. 16, p. 227–271.
- Thompson, J.H.F., Sillitoe, R.H., Baker, T., Lang, J.R., and Mortensen, J.K., 1999, Intrusion-related gold deposits associated with tungsten-tin provinces: *Mineralium Deposita*, v. 34, p. 323–334.
- Volkov, A.V., Sidorov, A.A., Goncharov, V.I., and Sidorov, V.A., 2002, Zoloto-sul'fidnyye mestorozhdeniya vkraplennykh rud Severo-Vostoka Rossii. Disseminated sulfide gold ore deposits in the Russian Northeast: *Geologiya Rudnykh Mestorozhdeniy*, v. 44, p. 179–197.
- Wallace, W.K., and Engebretson, D.C., 1984, Relationships between plate motions and Late Cretaceous to Paleogene magmatism in southwestern Alaska: *Tectonics*, v. 3, p. 293–315.
- Wilde, A.R., Layer, P., Mernagh, T., and Foster, J., 2000, The giant Muruntau gold deposit—why is it so large? [abs.]: *Geological Society of Australia Abstracts*, no. 59, p. 539.
- Yardley, B.W.D., 1997, The evolution of fluids through the metamorphic cycle, in Jamtveit, B., and Yardley, B., eds., *Fluid flow and transport in rocks—mechanisms and effects*: London, Chapman and Hall, p. 99–121.

